5650

OTS: 60-41,446 MAIN FILE JPRS: 5650

28 September 1960

RECORD COPY

SELECTED ARTICLES FROM

NEWS OF THE ASTROPHYSICAL INSTITUTE OF THE AN KSSR

RETURN TO MAIN FILE

Distributed by:

OFFICE OF TECHNICAL SERVICES
U. S. DEPARTMENT OF COMMERCE
WASHINGTON 25, D. C.

~~Price: $2.25~~

U. S. JOINT PUBLICATIONS RESEARCH SERVICE
205 EAST 42nd STREET, SUITE 300
NEW YORK 17, N. Y.

JPRS: 5650
C30: 4052-N

[Following is the translation of selected articles by various authors in Izvestiya Astrofizicheskogo Instituta AN KazSSR (News of the Astrophysical Institute of the Academy of Sciences of the Kazakh SSR) ~~vol~~ IX, ~~1959~~.] No 1960

POLARIZATION OF THE ZODIACAL LIGHT AS OBSERVED IN EGYPT (ASSUAN, OCTOBER TO NOVEMBER 1957)

pp 3-9 By V. G. Fesenkov

Photometric observations of the zodiacal light in southern Egypt, near the Tropic of Cancer, are especially favorable due not only to the exclusively clear and almost permanently cloudless sky, but also to the fact that the observations can be carried out twice during the same night, i.e., in the western part of the ecliptic shortly after sunset and in its eastern part shortly before dawn. Here, the evening and morning zodiacal lights are observed under entirely different conditions, although in essence they represent but different aspects of one and the same phenomenon. During the autumnal season, the morning zodiacal light is oriented normally toward the horizon and therefore can be observed up to the least possible angular distances from the Sun; it then appears exceedingly bright, in striking contrast to the comparatively weak evening zodiacal light as it spreads along the ecliptic strongly inclined to the horizon.

The great brightness of the eastern zodiacal light facilitates the carrying out of visual polarimetric observations of this phenomenon. Our visual binocular photometer /1/ was mounted in a manner to enable

its being easily fixed on any desired level convenient to the observer. It is equipped with an horizontal and a vertical circle having catches at intervals of 10°. It was possible to adjust the starting position of the horizontal circle in relation to Polaris; the exact position of the vertical circle was fixed at the start of the observations according to the level chosen.

For the polarimetric observations, the little objective lenses of the photometer were removed and polaroid plates inserted instead. Latters' position was adjustedin proper relation to the vertical. To this end, we used an auxiliary rectangular plate cut out from a similar polarcid polyvinyl film in such a manner that the polarization in the plate was directed parallel to its longest side.

In order to adjust the polaroids at the objective end of the photometer, the auxiliary polaroid plate was fixed vertically in such a manner that the direction of the long side of the rectangle coincided with the direction of the plumb line; next, each polaroid at the objective end was rotated until the field of view reached maximum obscurity, showing that at the given position of the objective polaroids their planes of polarization coincided with the vertical. Naturally, a setup of this kind is rather cumbersome at nighttime because of the general dimness of the heavens. This made it necessary to use a flashlight during the time before starting polarimetric observations of the morning zodiacal light. Adjustment of the polaroids before our nightly observations was effected in the twilight which proved bright enough

for this purpose.

Upon determining the initial orientation of the polaroids as above described, the measurements were performed at successive turns given to the polaroids by steps of 60° in the counterclockwise direction. The series of brightness measurements of a chosen point in the zodiacal light, obtained at three consecutive positions of the polaroid, beginning with the starting position indicated above, is sufficient to calculate the degree of polarization p and its angle of orientation α by using the conventional formulae:

$$p = 2\frac{\sqrt{j_1(j_1-j_2)+j_2(j_2-j_3)+j_3(j_3-j_1)}}{j_1+j_2+j_3} \qquad \text{A (4)}$$

and

$$\operatorname{tg} 2\alpha = \sqrt{3}\,\frac{j_3-j_2}{2j_1-j_2-j_3}, \qquad \text{B (4)}$$

where the angle α is counted from the starting psotion of the polaroids, that is, in this case, from the vertical line.

Obviously, the measurements to determine the polarization may be performed in purely relative units. The need for standarization arises only when we set ourselves the task to take account of such foreign sources of light as may be superposed on the zodiacal light. However, this problem is related to the more general problem of the reduction of photometric observations of the zodiacal light and will be examined by us in detail later on.

The Photometric Scale

In our binocular photometer which we were using in Egypt the photometric scale was determined by the motion of a wedge of almost neutral properties. The light from a small electric bulb or, as in the case of our observations in Egypt, from a luminophor* of steady luminescence, passes through a small lens and is converted into a pencil of parallel rays, which is then halved by means of a system of two rectangular prisms of total reflection. The two rather broad pencils obtained are redirected inside the visor tubes of the binocular photometer and are reflected into both eyes of the observer by means of two mirrors mounted at an angle of 45° at a distance of 12 cm from the eye-pieces. The orientation of the rectangular prisms and reflecting mirrors is so chosen as to ensure maximum uniformity of the reflected pencils of rays when the comparable areas in the field of view of the instrument represent uniformly lighted squares having an apparent size of approximately 3°. When observed with both eyes, these areas of comparison combine to form a single area situated in the center of the field of view.

The photometric wedge was first investigated as far back as in 1944, as is described in the book entitled "Meteoric Matter in Interplanetary Space" /2/. In this research, the photometric wedge was not dismantled at all, the investigation being conducted in a laboratory under ordinary working conditions, with the aid of an additional optical attachment. Another investigation of the said wedge was made in 1957 shortly before the expedition left for Egypt. The wedge was taken

* The Russian term for this artificial light source is "luminofor postoyannogo deystviya" (luminophor of constant action); it is described elsewhere in this collection as a luminary, in which the active surface is coated with a (phosphorescent) substance which shines with a steady light. Translator's note.

off and examined separately by means of a self-recording MF-4 microphotometer in the laboratory of the Astrophysical Institute of the Academy of Sciences of the Kaz. SSR. It should be noted that in the first investigation the zero point of the scale was determined merely by a stop in the photometer mounting preventing a further advance of the wedge. At the second investigation, the wedge end in its transparent part was taken as the zero point. This difference in zero-point fixation had to be taken into account when comparing the results of the two investigations.

The curves for the wedge scale in yellow and blue rays differ slightly from each other, the latter curve being somewhat steeper. However, this difference is inappreciable and, accordingly, an average curve may reliably be obtained; this would relate to green rays, corresponding to the maximum sensitivity of the eye.

Comparison of the 1947 (possibly 1944, cfr. above. Transl. note) and 1957 curves shows that they can easily be made to coincide, if the zero points are adjusted in a specific manner, notably, if they are shifted by 4.4 mm relative to each other. The true meaning of these shifts is easily established in the following manner. To start with, the photometer wedge is turned up to the stop and its position is marked on the recording tape connected with its mounting. Next, the wedge is so adjusted that its edge (which was taken as zero point in the second investigation) passes exactly through the middle of the area of comparison. In this case, a displacement of 3.3 mm and 5.6 mm, respectively, was found for the right-hand and left-hand tubes. The average

displacement of the wedge end from the stop thus amounted to 4.4 mm, that is, exactly as previously found by way of simple adjustment of the two photometric scales. However, an unexpected circumstance emerges here, namely: the zero points for the two visor tubes, corresponding to the right and left eye, do not coincide, but diverge by 2.3 mm. Let us check on whether this is apt to introduce any systematic errors in these measurements.

Suppose, for example, that for a series of scale readings, determined by the stop on the wedge mounting, we have the following brightness values expressed in certain relative units:

1	*2*	*3*	*4*
S=30 *mm*	2,88	33,3 *mm*	35,6 *mm*
31	2,76	34,3	36,6
32	2,64	35,3	37,6
33	2,53	36,3	38,6
34	2,41	37,3	39,6
35	2,30	38,3	40,6

The zero point set forth in the first column is the one actually used in these observations. The readings stated in columns 3 and 4 relate to the right and left eye, respectively, at a zero point coinciding with the bright end of the wedge.

For scale readings identical for both eyes we have the following brightnesses:

	Right eye	Left eye	Average	Former scale
$S=36$ *mm*	2,56	2,83	2,70	2,69
37	2,45	2,71	2,58	2,57
38	2,33	2,60	2,46	2,46

As is seen, the average of the readings for the left and right eye exactly coincides with that obtained when using the conventional working scale based on the support of the wedge mounting. This is clearly seen by comparison with the values given in the last column.

A similar satisfactory agreement is obtained even for the transparent front end of the wedge, where the movement of the scale differs appreciably from the linear one. Thus, e.g., we obtain in the same way the undernoted values for the transparent part of the wedge, starting from S = 16 mm:

	Right eye	Left eye	Average	Former scale
$S=16$ *mm*	5,71	5,84	5,77	5,80
17	5,60	5,80	5,70	5,73
18	5,45	5,74	5,60	5,62
19	5,27	5,64	5,46	5,47
20	5,09	5 50	5,30	5,29
21	4,91	5,33	5,12	5,11
22	4,72	5,15	4,94	4,93
23	4,53	4,96	4,74	4,74
24	4,34	4,77	4,56	4,55
25	4,16	4,58	4,37	4,36

The last column presents the scale readings in the case if the position of the wedge were the same for both eyes. Hence it is seen

that if the observations start at a value of S = 16 mm, the abovementioned slight divergence for both eyes is of no consequence whatsoever. For the polarization measurements we require only relative intensities at three consecutive positions of the polaroid. In view of this, we do not expound here the standarization methods applied by us. However, tabulated below is our final scale of the binocular photometer, expressed in absolute units. As the unit of brightness is taken that of a star of the 5th magnitude within a square of 1 degree of arc.

Photometric Scale

S	j	S	j	S	j	S	j
15 mm	10,72	30 mm	6,50	45 mm	3,33	60 mm	1,79
16	10,67	31	6,22	46	3,20	61	1,71
17	10,55	32	5,96	47	3,07	62	1,62
18	10,37	33	5,70	48	2,95	63	1,58
19	10,10	34	5,44	49	2,81	64	1,54
20	9,80	35	5,20	50	2,70	65	1,47
21	9,48	36	4,98	51	2,58	66	1,42
22	9,15	37	4,76	52	2,46	67	1,36
23	8,78	38	4,56	53	2,35	68	1,31
24	8,49	39	4,33	54	2,27	69	1,26
25	8,09	40	4,14	55	2,18	70	1,23
26	7,72	41	3,98	56	2,10	71	1,17
27	7,40	42	3,85	57	2,01	72	1,12
28	7,09	43	3,65	58	1,93	73	1,07
29	6,77	44	3,48	59	1,86	74	1,02
30	6,50	45	3,33	60	1,79	75	0,98

Under the conditions indicated above the determination of polarization represents quite a simple photometric problem. The only difficulty in the case of a visual photometer consists in the slight luminous intensity of the night sky and the consequential low degree of exactitude attainable with photometric instruments as compared, e.g., with photoelectric methods. Therefore, the data set forth below can-

not be regarded as final. They merely indicate the general characteristics of the phenomenon, which must be rendered more accurate by using more sensitive methods.

. For an example, consider the following observations:

Assuan, Libyan Desert

Longitude 32°51'.6, latitude 23°58'.9

October 24, 1957

Moscow time $19^h\ 32^m$; axis of zodiacal light at a distance of 100° west of Polaris. Height above the horizon 10°.

S_1	S_2	S_3	j_1	j_2	j_3	p	α
45,0	49,7	53,1	1,80	1,48	1,27	20,5%	--11°.7
47,7	50,3	51,8	1,61	1,44	1,34	10,8%	— 10,8
48,5	52,2	55,7	1,56	1,32	1,15	17,6%	— 12,5

October 26, 1957

Moscow time $5^h\ 34^m$; axis of zodiacal light *), height 10°.

S_1	S_2	S_3	j_1	j_2	j_3	p	α
46,8	59,0	51,2	1,67	1,33	1,38	14,1%	3°9
42,3	49,6	51,0	2,05	1,48	1,39	35,0%	—3,8
41,2	51,0	46,4	2,14	1,39	1,70	25,0%	12,1
41,9	47,5	46,0	2,09	1,62	1,73	22,7%	6,2
40,8	46,9	47,1	2,17	1,67	1,65	18,6%	—1,0

and so forth.

*) Apparent omission. Transl. note.

As is seen from the above, the various determinations of the degree of polarization differ substantially from each other, and only their mean values may be taken to correspond to reality. Nevertheless, even a cursory examination of the readings taken reveals an appreciable degree of polarization of the zodiacal light, as is apparent from the noticeable change in brightness caused by rotation of the polaroid.

Since the maximum brightness corresponds to the vertical position, i.e., to the starting position of the polaroid, it may be concluded that the orientation of the polarization differs but slightly from the vertical one.

h	ϑ	p	α	i	$h_\odot$
		24 October 1957,			
10^h	36°.4	16.3%	−11°.7	51°.0	−18°.0
		26 October			
10	28.3	23.2	3.5	87.7	−18.3
		27 October			
10	46.7	17.7	−8.2	88.4	−36.7
10	43.9	20.1	−2.9	88.5	−33.9
20	49.3	22.5	−2.9	88.4	−29.3
20	45.6	19.2	−2.8	88.2	−25.6
10	32.0	23.0	2.2	88.0	−22.0

1 November

20	78,9	16,6	—4,7	86,9	—58,9
10	66,4	15,9	—8,1	87,3	—56,4
10	62,6	15,8	—7,2	87,7	—52,6
10	57,4	13,0	—3,1	88,2	—47,4
10	54,4	10,1	—9,8	88,3	—44,4

16 November

10	40,9	21,7	—5,1	61,1	—25,4
10	44,8	18,9	—1,9	62,7	—29,3

20 November

10	33,7	18,4	—7,6	59,8	—18,9
10	35,8	16,1	—8,0	60,7	—21,0
20	50,0	22,9	—5,5	61,7	—23,6
30	64,0	16,5	—8,7	62,0	—25,8

The above Table gives averaged data for the degree of polarization p, the direction of the polarization vector α, as well as of various supplemental values characterizing the conditions of visibility of the zodiacal light, namely: the angular distance from the Sun of the observed point in the heavens and its height h above the horizon, the inclination i of the ecliptic to the horizon, and the submergence of the Sun below the horizon $h_\odot$.

A review of the data appearing in the Table allows of the following conclusions. The values of the degree of polarization diminish with the angular distance from the Sun, as is particularly clearly apparent in

the case of the morning zodiacal light. At an almost vertical position of the ecliptic the polarization vector differs little from the vertical and is almost exactly directed toward the Sun, as shown by the attached figure relating to October 27th.

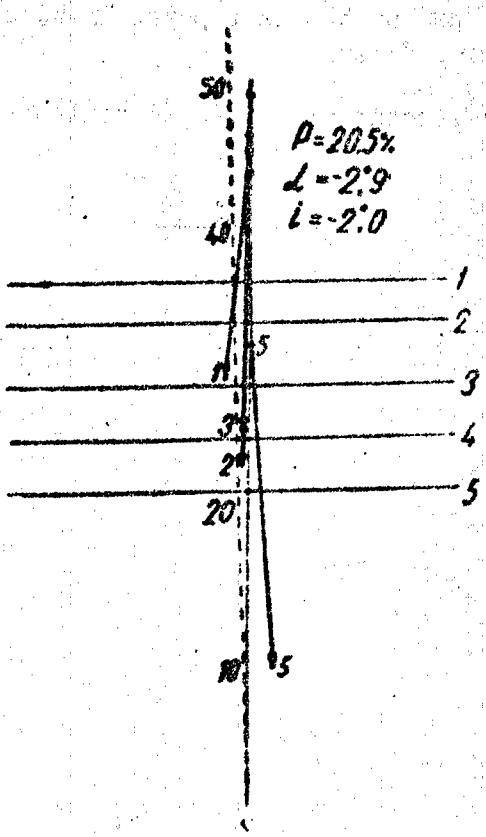

Fig. 1

Allowance for superposed foreign light sources, even nonpolarized ones, cannot in the case of the morning zodiacal light substantially affect the magnitude of the polarization found. However, an explanation is wanted for the peculiar fact that the direction of the polarization vector deviates appreciably from the direction toward the Sun and, at

considerable inclinations of the ecliptic, relative to the horizon. This circumstance requires special verification by means of more accurate photoelectric observations.

References

1. V. G. Fesenkov, "News of the Astrophys. Inst. of the Ac. of Sci. Kaz. SSR", 1958, vol VII.

2. V. G. Fesenkov, "Meteoric Matter in Interplanetary Space", Moscow, 1947.

ON THE METHOD OF REDUCING PHOTOMETRIC OBSERVATIONS OF ZODIACAL LIGHT

pp 35-39 By V. G. Fesenkov

It is known that the apparent brightness of the zodiacal light, particularly of its less luminous parts, represents a complex phenomenon depending on several different components, namely:

(a) The stellar, or, more generally, the galactic component; it is constituted by the integral light of the stars of our Galaxy diffused in interstellar space as well as in the terrestrial atmosphere, predominantly in the troposphere;

(b) The ionospheric component which, properly speaking, constitutes the luminescence of the night sky and depends on various light sources of terrestrial origin; it is characterized by emission lines and bands and by a continuous spectrum. The light diffused in the troposphere is a contributing factor.

(c) The third component, which is distributed extremely ununiformly over the entire firmament, depends on the zodiacal light both observed directly and diffused, chiefly, in the troposphere. Under this head may also be classed the so-called zodiacal twilight which is due to the illumination of the atmosphere near the horizon by the brighter regions of zodiacal light already hidden below the horizon but producing a faint crepuscular effect.

The problem is to find the right system of isophots that would characterize the phenomenon of zodiacal light in such a way as it would be observed outside the atmosphere and detached from the background presented by our Galaxy.

It would be too crude an approach to this problem if we should attempt to reduce the observations of the zodiacal light by simply deducting from the observed brightness the celestial background on the same almucantar taken at the proper distance from the ecliptic. Indeed, the zodiacal light is spread over the entire vault of heaven, which is evident, inter alia, from the fact that the Earth moves within the medium constituted by the interplanetary matter that diffuses the light of the Sun. For this reason, even at distances of several tens of degrees from the ecliptic one observes some change in brightness of zodiacal origin. Moreover, with such a method of reduction it is impossible to match the brightness of the sky on different almucantars. Yet it is bound to vary in a definite manner according to the effective height of the layer responsible for the luminenscence of the ionosphere. Finally, this method does not adequately allow for the variation in the galactic component and takes no account at all of the nonuniformity of illuminance of the nocturnal sky caused by the tropospheric scattering of the zodiacal light itself.

Below, we are going to expound the method of reduction of photometric observations of the zodiacal light adopted by us.

In order to account for the variability of the illuminance due

to the ionospheric component it is recommended during the observations to keep track of the brightness of the night sky preferably near to the celestical pole, where the configuration of the stars and the zenithal distance are always the same for a given observation.

Next, from the observed brightness of the heavens near to the pole, relating to a specific region of the spectrum and expressed in definite absolute units (e.g., the number of stars of the 5th magnitude per square degree of arc), we subtract the galactic component corrected for the atmospheric absorption of light and for the scattering of the galactic light in the troposphere in dependence on the transparency factor. This reduction is inappreciable. It can be presented in the form of the approximated Expression:

$$L(b)\cdot p^{\sec z} + 0{,}355\,\varphi(\overline{z,z_i})\,\sec z_i\left(1-\frac{1}{4}\sin^2 b\right), \qquad (1)$$

where b is the galactic latitude;

z_i is the zenithal distance of the celestial point observed, and

L (b) is the integral light of the stars in the given region.

The additive term in this Expression is rather small, as may be seen from the following comparison:

$\sec z_i$	1	1,5	2	3	4	6
$p=0{,}83$	0,050	0,072	0,091	0,114	0,152	0,191
$p=0{,}86$	0,042	0,062	0,079	0,110	0,136	0,179

In Table 1 we state the value of the component giving the correction for the integral brightness of the stars and its scattering in the troposphere according to Expression (1) /3/.

Table 1

z \ b	0	10	20	30	40	50	60	70	80	90
0°	1,68	1,21	0,85	0,58	0,41	0,30	0,24	0,23	0,21	0,21
10	1,67	1,22	0,86	0,58	0,40	0,29	0,24	0,23	0,21	0,22
20	1,66	1,21	0,85	0,59	0,41	0,29	0,24	0,23	0,21	0,22
30	1,64	1,19	0,84	0,58	0,41	0,30	0,24	0,22	0,22	0,21
40	1,59	1,16	0,82	0,57	0,39	0,29	0,24	0,23	0,22	0,21
50	1,56	1,14	0,81	0,56	0,39	0,29	0,24	0,22	0,22	0,22
55	1,53	1,12	0,80	0,55	0,39	0,29	0,24	0,23	0,21	0,21
60	1,47	1,08	0,77	0,54	0,38	0,29	0,26	0,23	0,21	0,21
65	1,41	1,04	0,75	0,53	0,38	0,28	0,26	0,23	0,21	0,21
70	1,31	0,97	0,70	0,51	0,37	0,29	0,25	0,23	0,22	0,21
75	1,17	0,88	0,65	0,48	0,35	0,28	0,24	0,23	0,22	0,22
80	0,95	0,74	0,56	0,43	0,33	0,28	0,24	0,23	0,22	0,22

At large galactic latitudes the decrease of the first term is almost exactly compensated for by the increase in the second term and, consequently, on balance the galactic correction remains unchanged. Contrariwise, near the galactic plane it is appreciable and therefore unreliable. Local absorption in individual galactic clouds may considerably change its value. For an example, we may indicate the region of the sky around Polaris. According to the data of Table 1, the galactic reduction, e.g., at $z = 47^\circ$ and $b = 30^\circ$, equals 0.56, whereas it should be taken as equal to 0.38, the difference being due to considerable light absorption in the cosmic clouds surrounding the region around the celestial pole.

It should be noted, further, that at an inclined position of the Milky Way relative to the horizon of the observer the data of Table 1 have to be somewhat reduced. Finally, it is necessary to allow for the presence of the zodiacal component at the same point, that is, around the celestial pole. About its value various authors have expressed extremely divergent opinions. No doubt, it is very difficult to determine its magnitude by purely photometric methods, because the result entirely depends on the transparency factor. A much more reliable way is to evaluate the zodiacal component by means of polarimetric measurements with the aid of certain theoretical considerations.

Suppose we are observing the complex effect produced by the presence of two differently polarized brightness components I and I_1 and of the degrees of polarization P and P_1. The angle of preferential polarization between the two components we will designate by α_1. Let I_m and P_m be the observed total values of brightness and the degree of polarization, respectively. Let us further designate by α_m the angle between the vector of the total polarization and the first component.

We then have the following Equations / 4 / :

$$(I_m P_m)^2 = (IP)^2 + (I_1 P_1)^2 + 2 IP\, I_1 P_1 \cos 2\alpha_1,$$
$$(I_1 P_1)^2 = (I_m P_m)^2 + (IP)^2 - 2 I_m P_m IP \cos 2\alpha_m,$$

which correspond to a linear triangle with the sides IP, $I_1 P_1$, and $I_m P_m$ and the angles: between I P and $I_1 P_1$ equal to $2\alpha_1$, and between $I_m P_m$ and I P, equal to $2\alpha_m$.

Assuming, as is the case in reality, that the polarization of the ionospheric luminescence as well as of the galactic component is very close to zero, then with P_m as the observed total polarization around the pole we have

$$I_1 P_1 = I_m P_m,$$

whence

$$I_1 = I_m \frac{P_m}{P_1},$$

where P_1 is the polarization of the zodiacal component about the pole, which can easily be found by theoretical reasoning. The value obtained is roughly the same for different models simulating the scattering of light within the complex of zodiacal matter.

By order of magnitude, this polarization is approximately the same as in the ecliptic plane at an angular distance from the Sun of about 30°.

Hence, if the factually observed polarization in the polar region is of the order of 1-2%, while the true polarization of zodiacal light

in the same plane should be not less than 20%, it follows that the zodiacal component in point of brightness constitutes not more than 5% of the total observed brightness and, essentially, may be neglected.

In evaluating the zodiacal component in the region of the celestial pole (in case it has been more accurately determined) and knowing the magnitude of the galactic component at the same point, then as wasdiscussed above, we are able to single out at this point from the observed total brightness only that part which is caused by the ionosphere.

It may be assumed that this ionospheric component is distributed over the celestial sphere with some degree of regularity. As was repeatedly pointed out earlier, the luminescence of the ionosphere can be represented with sufficient accuracy on the assumption of the existence of only one luminescent layer having an effective height of 200 to 250 km /5/. In reality, the luminescence of the nocturnal sky due to the ionosphere is of a somewhat tufty nature, but it is not possible to take into consideration suchlike irregularities which, moreover, are of a passing nature.

Apart from that, it can be shown /7/ that the tropospheric scattering of this component can with sufficient accuracy be accounted for simply by increasing the transparency factor by 0.03. In the final analysis, this component, including also the portion of its light scattered in the troposphere, can be represented in the form of the simple Expression

$$\frac{C(p+0{,}03)^m}{\sqrt{(1+h)^2-\sin^2 z}},$$

where h denotes the effective height of the ionospheric layer in units of the Earth's radius, and C is a variable factor which may change both with time and the position of the observer. Essentially, it must be determined in the course of the observations.

Thus, supposed we know around the celestial pole the value of the ionospheric component corresponding to the zenithal distance z_0, we may reduce it to any other zenithal distance z by multiplying it by the factor

$$(p+0{,}03)^{\sec z-\sec z_0}\sqrt{\frac{(1+h)^2-\sin^2 z_0}{(1+h)^2-\sin^2 z}}.$$

Added to this the galactic component which is found from our tables for the observed point of the zodiacal light, allowing for its light scattered in the troposphere, and, finally, the tropospheric luminescence due to the extensive dimensions of the zodiacal light, we

find by way of final reduction the value which it is necessary to deduct from the observed brightness.

Hence, the reduction value to be subtracted from the observed brightness at a given point of the zodiacal light is as follows:

$$\text{Red} = (\, I_0 - \text{gal. comp. at pole} - \text{zod. comp. at pole}\,) \times (\, p + 0.03\,)^{\sec z - \sec z_0} \sqrt{\frac{(1+h)^2 - \sin^2 z_0}{(1+h)^2 - \sin^2 z}}$$

+ gal. comp. (Z, l, b) + zod. comp. in trop.

Finally, the true brightness of the zodiacal light, allowing for absorption in the terrestrial atmosphere, is

$$(I_{app} - \text{Red})\, p^{-\sec z}.$$

It must be noted that to be able to find the abovementioned reductions one must keep a constant watch over the optical properties of the Earth's atmosphere. In particular, one has to know the value of the transparency factor, which varies from one day to the other. The indicatrix of scattering is also needed for evaluating the tropospheric illuminance, especially that produced by the zodiacal light itself. However, in the given case we may restrict ourselves to the standardized form found from numerous observations.

References

1. V. G. Fesenkow, "Meteoric Matter in Interplanetary space", Moscow 1947, pp 212 amd 257.

2. Id., op. cit. p 203, Table 29.

3. Id., op. cit. p 258, Table 38.

4. Id., "Astronomical Journal", 1958, vol 35, ed. 5.

5. D. Barbier - Ann. de Géoph., vol 12, p 144, 1945

6. Id. "Vistas in Astronomy", vol 2, p 929, London, 1956.

7. V. G. Fesenkov, "Meteoric Matter in Interstellar Space", Moscow, 1947, p 195.

ON THE PROBLEM OF DETERMINING THE NOCTURNAL TRANSPARENCY FACTOR

pp 53-55 by A.V. Kharitonov

It is known that by Buger's method we can only obtain the value of the transparency factor provided the latter remains constant during the whole period of observation. If it varies, this method is altogether inapplicable, since at nonuniform variation of the transparency Buger's line cannot be a straight line. On the other hand, in the case of uniform variation, e.g., an increase with time, Buger's line, while following a straight course, is bound to change its inclination in such a manner that the value of the transparency factor turns out too low in the observation of a rising star and too high in that of a setting star.

This difficulty can be overcome by observing two stars, one rising and one setting, in order to compensate for the drop in the transparency factor in the first case by the rise occurring in the second case, or else by observing one star before and after culmination. However, these methods yield only the mean value of the transparency factor over a prolonged period of time (3 to 5 hours), which does not come up to the requirements of accurate stellar photometry. Indeed, it is required that we know the transparency factor at any instant during observation.

To determine it, let us observe at different zenithal distances

a certain star α which at the instants $t_i \ldots, t_k \ldots, t_n$ emits to us the luminous fluxes $I_i \ldots, I_k \ldots, I_n$, respectively. Suppose that at the same time we are observing a star N near the celestial pole, whose zenithal distance we will in the first approximation consider invariable. Suppose this star emits to us, at the same instants, the luminous fluxes $i_i \ldots, i_k \ldots, i_n$. In the case of photoelectric observations, the values I_k and i_k may be simply substituted by the galvanometer readings upon correcting the latter according to standard readings for variations with time of the sensitivity of the instrument.

If the i_k values do not differ from each other, then the transparency is constant. If they do, that means that the transparency varies. Indeed, the zenithal distance of the star N is constant and the variation of the instrument's sensitivity has been allowed for. In the first case, one can obtain the value of the (constant) transparency factor by processing the results of observation of the star according to Buger's method; in the second case, we shall proceed as follows.

Let us find the mean of the values $\frac{i_k}{i_c} = \frac{\sum_{k=1}^{n} i_k}{n}$. Since the i_k values were received at roughly equal time intervals, the quantity i_c will correspond, for the time of observation, to the mean value of the transparency factor p_c, while the i_k values will correspond to p_k instantaneous values of it at the instants t_k.

We have

$$i_k = i_0 \cdot p_k^{M(z)}, \qquad (1)$$

$$i_c = i_0 \cdot p_c^{M(z)}, \qquad (2)$$

where i_o is the extraatmospheric flux from the star N and M(z) is the mass of air (constant in the first approximation) through which the star is being observed. From Formulae (1) and (2) we obtain:

$$\frac{p_c}{p_k} = \left(\frac{i_c}{i_k}\right)^{\frac{1}{M(z)}}. \qquad (3)$$

For the star α, at the instant t_k, we have:

$$I_k = I_0 \cdot p_k^{M(z_k)}, \qquad (4)$$

where I_o is the extraatmospheric flux. Let us reduce all I_k values to the so far unknown mean value of the transparency factor p_c. The reduced flux I'_k is equal to

$$I_k' = I_0 \cdot p_c^{M(z_k)}. \qquad (5)$$

From the Equalities (4) and (5) we obtain

$$I_k' = I_k \left(\frac{p_c}{p_k}\right)^{M(z_k)}, \qquad (6)$$

whence, considering (3), we have

$$I_k' = I_k \left(\frac{i_c}{i_k}\right)^{\frac{M(z_k)}{M(z)}}. \qquad (7)$$

All values in the right-hend part of this Formula are known to us. Upon reducing with the aid of this Formula all I_k values to the mean transparency factor, we are able to construct a Buger line, now utilizing the value I_k which gives us the value p_c.

Thereafter, using Formula (3), it is easy to determine any momentary value of the transparency factor p_k.

The proposed method does not take account of the azimuthal effect on the transparency of the atmosphere. Mention should, however, be made of the observations conducted over many years by Ye. V. Pyaskovskaya-Fesenkova at the observatory of the Astrophysical Institute. These observations which, it is true, were carried out during the daytime, prove that in cloudless weather the azimuthal effect is absent. Furthermore, this effect is not being allowed for in all other known methods for determining the transparency factor, except the method of B. V. Nikonov. However, it seems to us that our method is simpler.

It should be noted that in observations using wide-band filters the stars N and α should have the same energy distribution in the spectrum, i.e., the same color index.

Among the circumpolar stars, the following two may be recommended for these observations:

(1) A (54)

This star is listed in the NSP under No. 5; for it

$$m_{I_{pv}} = 6.^m 46; \quad c^I = 0.^m 00.$$

(2) B (54)

This star is listed in the NSP under No. 6; for it

$$m_{I_{pv}} = 7.^m 08; \quad c_I = 0.^m 07.$$

The stars indicated are sufficiently luminous and are suitable

for photometric measuring. Both are very close to the celestial pole, so very little correction is necessary for change of altitude. Also, due to the coordinates of these stars, one of them almost invariably keeps within such angular positions (about 0 or 12^h) that its altitude remains virtually constant for the duration of the observation.

A SPECTROPHOTOMETRIC INVESTIGATION OF THE CONTINUOUS AND EMISSION SPECTRA OF THE NIGHT SKY IN THE VISUAL REGION OF THE SPECTRUM

Pp 86-95

By Ye. V. Karyagina and
L. N. Tulenkova

At the present time, the energy distribution in the continuous spectrum of the night sky, in absolute units, is not yet known. Data given in a recently published manual by Allen / 1 / have been obtained by evaluating the results of Babcock's and Johnson's observations /2/. These authors obtained spectra of the night sky in a monoprismatic quartz spectrograph having a dispersion near H_γ of 1100 A/mm; it is equipped with a Schmidt camera (aperture ratio 1/1). The instrument was used in combination with a 12 inch Cassegrain reflecting telescope of the Mt Palomar observatory (exposition time 10 hours). A standard incandescent bulb with known color scale, whose spectrum was obtained at an exposure of only 30 sec, was used for standardization. The difference in exposure time necessitated reductions which could have become the source of systematic errors; because of that, Allen's results can hardly be considered sufficiently accurate.

The photoelectric investigations by K. K. Chuvayev /3/, which appear to be more reliable, cover only a narrow range of wavelengths between 4700 and 5600 A.

We made an attempt to determine the energy distribution in the

continuous spectrum of the night sky and to evaluate its importance relative to the emission spectrum. For this purpose we used spectrograms obtained in September and October with the aid of a G A I S H *) type powerful nephelometric spectrograph which was then installed in the region of Lake Bolshoye Almatinskoye (H ≃ 3000 m). Its optic power (aperture ratio 1/0.7) and inconsiderable dispersion (2600 A/mm near λ 5600A) made it possible to obtain sufficiently dense negatives of the continuous spectrum of the night sky on OaF plates (British Kodak) at 30^m exposure and a spectrograph slit width of 4 mm. Usually, the emission lines obtained were not overexposed. For calibration purposes we used four luminophors of steady luminescence attenuated by several neutral filters /4/. For standardization, we took the spectra of δ Cygni and ζ Draconis at the same exposure and at the same zenithal distance (z=47°) as for the sky spectrum. For one day of observation, notably September 28-29, the energy distribution was measured using α Lyrae for its determination in relative units; the tie to absolute units was made with the aid of a luminophor of steady luminescence, whose spectrum was obtained simultaneously with those of the sky. The energy distribution in the celestial spectrum in the range of wavelengths between 4400 and 6400 A had previously been investigated in absolute units by N. N. Pariyskiy and L.M. Gindilis /5/.

---

*) Manufacturer's trade mark. Transl. note.

The transparency of the atmosphere was determined for each night of observation from 4 - 5 photographs of star spectra at different zenithal distances by Buger's method, the spectra of δ Cygni and α Lyrae being used for the purpose. The transparency factor was established for 12 wavelengths ranging from 4000A to 6400 A. It is graphically represented on Fig. 1, as a function of the wavelength, for three days of observation. In the evaluation of our observations on September 28/29 we utilized the mean transparency factor ascertained by us for September 27/28 and 29/30.

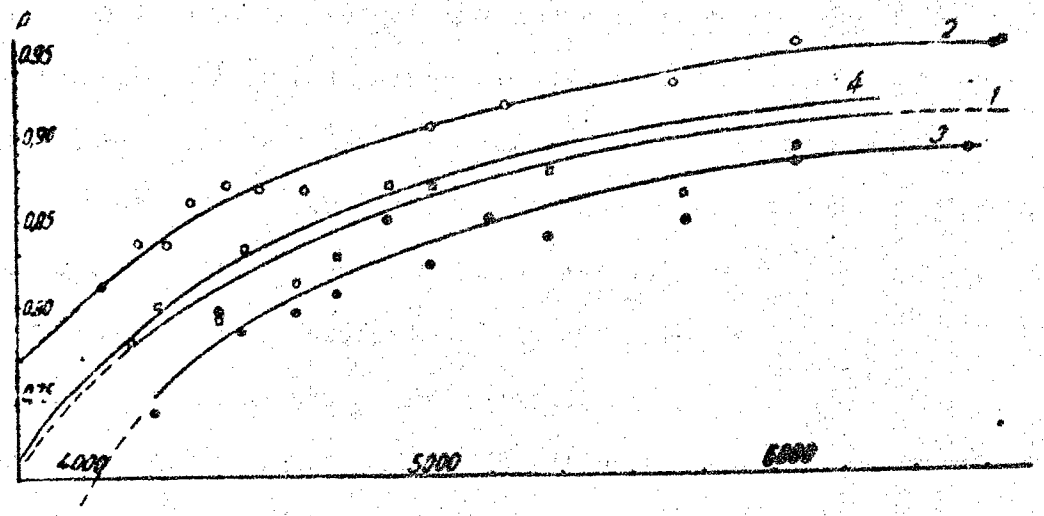

Fig. 1. Legend: □ Sep 27/28, 1957 - curve 1; ○ Sep 29/30, 1957 - curve 2; ● Sep 23/24. 1957 - curve 3; observations in Montezuma - curve 4.

In view of the considerable scattering of observational points we relied for plotting the P (λ) curves on the transparency distribution at a wavelength determined by Abbot /6/ from observations made in Mon-

tezuma ($H \simeq 2700$ m). See curve 4 in Fig. 1.

In all, we evaluated 7 spectrograms of the night sky, of which 5 related to the circumpolar region and 2 to the region near β Draconis.

The spectrograms were measured on an MF-2 microphotometer at intervals of 0.01 mm along the spectrum; width of the slit in front of the photocell 0.3 mm; magnification 30 $\times$.

Calibration curves were constructed for the wavelengths 6400; 6100; 5600; 5100; 4762; 4400; and 4300 A from 3-4 photographs of the luminary's spectrum, which were taken at a width of the spectrograph slit varying from 3 to 8 mm.

The calibration curves, averaged in the wavelength intervals $1300 < \lambda < 4800$, $4800 < \lambda < 5100$, $5100 < \lambda < 6400$ A, were utilizable for these intervals with a sufficient degree of accuracy.

As indicated above, our observations aimed at obtaining the energy distribution in the continuous spectrum of the nocturnal sky $I_s(\lambda)$ and determining the intensity of the emission lines 5577, 5893, 6300 + 6364 A, using for standardisation such stars whose energy distribution $I_*(\lambda)$ is known.

The basic formula can be obtained proceeding from the following simple reasoning. Within the wavelength interval λ and $\lambda + \Delta\lambda$, the energy per 1 cm^2 of the Earth's surface emanating from 1 sq. degree of the celestial sphere equals $I_s(\lambda)\, d\lambda$, while that from the reference star equals $I_*(\lambda)\, p^{m(z)}\, d\lambda$. On the spectrograms taken with the

nephelometric spectrograph the image of the star appears as a small strip whose width depends on the instrumental contour of the spectrograph and whose height is determined by the solid angle ω of the collimator. Consequently, the illuminance on the photographic plate produced by a section of the sky with a solid angle ω in the wavelength interval $d\lambda$ is equal to

$$b_s(\lambda)\,d\lambda = I_s(\lambda)\,\omega\,\Phi(\lambda)\,\frac{\Delta}{k}\,d\lambda, \qquad (1)$$

and that produced by the reference star is equal to

$$b_*(\lambda)\,d\lambda = I_*(\lambda)\,p^{m(z)}\,\Phi(\lambda)\,\frac{\Delta}{k}\,d\lambda, \qquad (2)$$

where $b_s(\lambda)$ and $b_*(\lambda)$ are the observed illuminances from the sky and the reference star;

$\Phi(\lambda)$ is the selective sensitivity of the instrument;

Δ is the width of the slith; and

K is the magnification factor;

$$\omega = \frac{\pi d^2}{4f^2} \text{ radian} = 0.983 \text{ sq. degree}$$

where d is the collimator diameter, and

f is its focal length.

The spectrum of the star appears on the plate as a strip about 0.45 mm wide, which corresponds to a mean angle of about 1° of arc on the celestial sphere. Manifestly, superposed on the star spectrum is background radiation from the continuous spectrum of the night sky, which is also visible on both sides of the star spectrum (Fig. 2).

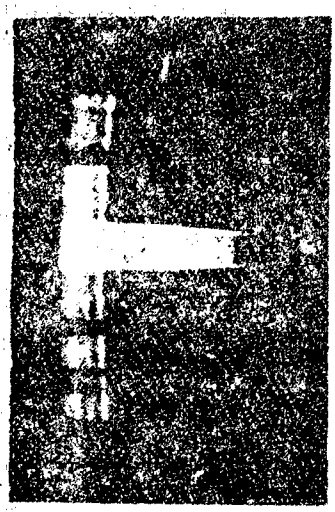

Fig. 2

From Eqs. (1) and (2) we find

$$\frac{b_s(\lambda)}{b_*(\lambda)} = \frac{I_s(\lambda)\,\omega}{I_*(\lambda)\cdot p^{m(z)}}. \qquad (3)$$

In evaluating the spectrograms of the reference stars we measured photometrically the spectra of the stars and the sky spectrum on either side of each star. The densities obtained were smoothed out graphically; thereupon, the observation values for the "star plus sky" intensity $b_{s+*}(\lambda)$ and the mean-sky intensity $b_s(\lambda)$ were found in the usual way from the calibration curves. The observed intensities for the reference stars themselves were by difference, as below:

$$b_*(\lambda) = b_{s+*}(\lambda) - b_s(\lambda).$$

It is evident from Formula (2), that in order to obtain the energy distribution within the sky spectrum in absolute units, the quanti-

ty $I_*(\lambda)$, too, must be known in absolute units. The energy distribution in the spectrum of the reference star was known to us in relative units $i_*(\lambda)$ only, i.e., with an accuracy up to the constant factor, not depending on the wavelength,

$$I_*(\lambda) = C \cdot i_*(\lambda). \qquad (4)$$

The constant C can be found provided we know the difference between the visual stellar magnitudes of the Sun and the referance star, as well as the energy distribution in the solar spectrum in absolute units.

Let $I_\odot(\lambda)$ and $I_*(\lambda)$ be the spectral illuminances from the Sun and the reference star outside the boundry of the atmosphere, and $V(\lambda)$ - the visibility function.

$$\frac{\int_0^\infty I_*(\lambda)\, V(\lambda)\, d\lambda}{\int_0^\infty I_\odot(\lambda)\, V(\lambda)\, d\lambda} = 2{,}512^{m_\odot - m_*}, \qquad (5)$$

where $m_\odot$ and m_* are the visual magnitudes of the Sun and the reference star. We know the mean spectral radiation intensity $F_\odot(\lambda)$ of the Sun (no allowance made for absorption lines and for the average emission of the entire solar disc) in absolute units /7/. Then

$$I_\odot(\lambda) = \frac{\pi r_\odot^2}{a^2} F_\odot(\lambda) = \pi F_\odot(\lambda) \sin^2 r'_\odot, \qquad (6)$$

where $r_\odot$ is the linear solar radius;

$r'_\odot = 16$ min is the angular solar radius at the mean distance of the Earth from the Sun:

a is the major semiaxis of the Earth's orbit.

From Eqs. (4), (5) and (6) we get

$$C = \pi \sin^2 r'_\odot \cdot 2{,}512^{\,m_\odot - m_*} \frac{\int_0^\infty F_\odot(\lambda)\, V(\lambda)\, d\lambda}{\int_0^\infty i_*(\lambda)\, V(\lambda)\, d\lambda}. \qquad (7)$$

The quantities required for calculating the integrals in Formula (7) for the two reference stars, viz., δ Cygni and β Draconis are found in Table 1.

Column 2 of Table 1 gives the energy distribution in the spectrum of δ Cygni in relative units, calculated from Planck's ratio, taking the star's temperature as equal to 11 900° (according to Brill /8/); column 3 gives the spectral energy distribution for β Draconis according to Kienle, Wempe and Beilicke /9/; column 4 gives $F_\odot(\lambda)$ in erg/cm^2 · sec · sterad · $\Delta\lambda$ = 1 cm; column 5 – the visibility factor $V(\lambda)$; and columns 6,7,8 – the products $i_*(\lambda) \cdot V(\lambda)$ and $F_\odot(\lambda) \cdot V(\lambda)$.

The stellar magnitude of the Sun, needed for calculating the constant C is taken /10/ as

$$m_\odot = -26{,}^m72 \pm 0{,}03.$$

The magnitudes of the reference stars, according to the international photovisual scale /11/, are: $m_{\beta Dra} = 2.^m75$ and $m_{\delta Cyg} = 2.^m87$.

The values obtained for C, as calculated from Formula (7), were:

$C_{\delta Cyg} = 3{,}01 \cdot 10^{-2}$ erg cM^2 sec units $i_*(\lambda)_{\delta Cyg}$;

$C_{\beta Dra} = 1{,}38 \cdot 10^{-2}$ erg cM^2 sec units $i_*(\lambda)_{\delta Dra}$.

Table 1

λ	$i_*(\lambda)$		$F_\odot(\lambda)$	$V(\lambda)$	$i_*(\lambda)V(\lambda)$		$F_\odot(\lambda)V(\lambda)$
	δ Cyg	β Dra			δ Cyg	β Dra	
1	2	3	4	5	6	7	8
4000	1,868	1,14	$21{,}2\times10^{13}$	0,0004	0,001	0,000	$0{,}01\times10^{13}$
4100	1,783	1,32	25,8	0,0012	0,002	0,002	0,03
4200	1,703	1,39	26,8	0,0040	0,007	0,006	0,11
4300	1,627	1,49	26,4	0,0116	0,019	0,017	0,31
4400	1,552	1,67	27,7	0,0230	0,036	0,038	0,64
4500	1,481	1,78	29,8	0,0380	0,056	0,068	1,13
4600	1,412	1,93	30,9	0,0600	0,085	0,116	1,85
4700	1,347	2,04	31,3	0,0910	0,123	0,186	2,85
4800	1,285	2,17	31,1	0,1390	0,178	0,302	4,32
4900	1,226	2,21	30,9	0,2080	0,255	0,460	6,43
5000	1,171	2,13	30,3	0,3230	0,378	0,680	9,79
5100	1,117	2,06	29,6	0,5030	0,562	1,036	14,90
5200	1,066	2,04	28,8	0,7100	0,757	1,448	20,45
5300	1,017	2,10	28,2	0,8620	0,877	1,810	24,31
5400	0,971	2,17	27,6	0,9540	0,927	2,070	26,33
5500	0,927	2,24	27,3	0,9950	0,922	2,229	27,16
5600	0,886	2,29	27,1	0,9950	0,882	2,279	26,96
5700	0,847	2,30	27,0	0,9520	0,806	2,190	25,70
5800	0,809	2,30	27,1	0,8700	0,704	2,000	23,58
5900	0,773	2,31	27,1	0,7570	0,585	1,749	20,51
6000	0,740	2,28	26,6	0,6310	0,467	1,439	16,78
6100	0,780	2,21	25,6	0,5030	0,356	1,112	12,89
6200	0,677	2,23	24,8	0,3810	0,258	0,850	9,45
6300	0,648	2,22	24,3	0,2650	0,172	0,586	6,44
6400	0,620	2,20	24,0	0,1750	0,109	0,385	4,20
6500	0,594	2,19	23,8	0,1070	0,064	0,234	2,55
6600	0,569	2,18	23,6	0,0610	0,035	0,133	1,44
6700	0,545	2,16	23,4	0,0320	0,017	0,069	0,75
6800	0,523	2,12	22,9	0,0170	0,009	0,038	0,39
6900	0,501	2,10	22,3	0,0082	0,004	0,017	0,18
7000	0,481	2,08	21,7	0,0041	0,002	0,008	0,09
7100	0,462	2,06	21,0	0,0021	0,001	0,004	0,04
7200	0,443	2,00	20,3	0,0010	0,000	0,002	0,02

Hence, knowing C , we can determine $I_*(\lambda)$, i.e., the illuminance from the reference stars outside the atmosphere. The results are set forth in Table 2, where column 1 gives the wavelengths; the remaining columns show the monochromatic illuminances from the reference stars outside the atmosphere and from the luminophor in erg/cm^2·sec·sterad·$\Delta\lambda$ = 1 cm. The $I_*(\lambda)$ values for α Lyrae were taken from ref. /5/.

Using the $I_*(\lambda)$ values from Table 2, it is possible from Formula (3) to find $I_s(\lambda)$ in erg/cm^2·sec · sq. degr. $\Delta\lambda$ = 1 cm.

In Tables 3 and 4 are presented the observed intensity values $b_*(\lambda)$, $(b_p(\lambda))$ and $b_s(\lambda)$ for all reference stars, and the value $b_p(\lambda)$ for the luminophor, covering all 7 spectrograms of the sky. Column designations in these Tables are: column 1 - wavelengths, all other columns - values of the observed intensities. The observed illuminances for the reference stars have been corrected for atmospheric absorption.

The final results of the study of energy distribution in the continuous spectrum of the night sky for the circumpolar region and the region around β Draconis for all 7 spectrograms taken are presented in Table 5 (in erg/cm^2 . sec · sterad · $\Delta\lambda$ = 1 A × 10^7). To obtain these, the $I_s(\lambda)$ values calculated from Formula 3 have to be multiplied by 3283 · 10^{-8}.

Table 2

λ	$I_s(\lambda)$			Luminophor
	β Dra	δ Cyg	α Lyr	
1	2	3	4	5
4000	0,0157	0,0563	0,808	
4100	0,0182	0,0 37	0,784	
4200	0,0192	0,0513	0,783	
4300	0,0206	0,0490	0,734	
4400	0,0230	0,0467	0,685	
4500	0,0246	0,0446	0,642	$7,51 \cdot 10^2$
4600	0,0266	0,0425	0,599	8,20
4700	0,0282	0,0405	0,555	10,8
4800	0,0299	0,0387	0,515	17,6
4900	0,0305	0,0369	0,475	7,90
5000	0,0294	0,0352	0,454	8,06
5100	0,0284	0,0356	0,439	8,47
5200	0,0282	0,0321	0,426	8,59
5300	0,0290	0,0306	0,407	8,30
5400	0,0299	0,0292	0,388	7,89
5500	0 0309	0,0279	0,368	6,79
5600	0,0316	0,0267	0,352	6,07
5700	0,0317	0,0255	0,334	5,77
5800	0,0317	0,0243	0,316	5,36
5900	0,0319	0,0233	0,299	4,95
6000	0,0315	0,0223	0,284	4,62
6100	0,0305	0,0213	0,267	4,05
6200	0,0308	0,0204	0,252	3,62
6300	0,0306	0,0195	0,236	3,33
6400	0,0304	0,0187	0,222	3,56
6500	0,0302	0,0179	0,205	

In Table 5 are given – in column 1: wavelengths; in columns 2 thru 8: $I_s(\lambda)$ values for all 7 spectra; in column 9: mean energy distribution according to the first 5 spectra (a to e) obtained for the region around the celestial pole. It should be noted that the $I_s(\lambda)$ spectra obtained on Sep 29/30 differ appreciably from all others both by the intensity of the $I_s(\lambda)$ values and by the energy distri-

Table 3

λ	δ Cyg	α Lyr	β Dra	β Dra	Luminophor 28/29.IX	
	27/28.IX	28/29.IX	29/30.IX	23/24.X	Spec- 3 trum	Spec- 4 trum
1	2	3	4	5	6	7
4100		16,1	8,2	9,3		
4200	27,4	17,2	10,3	9,6		
4300	28,7	18,0	12,7	10,4	2,8	2,4
4400	28,4	18,6	14,8	12,0	3,9	3,1
4500	26,9	18,4	17,8	14,5	4,8	3,7
4600	24,8	17,6	19,7	14,9	4,83	3,8
4700	22,2	16,1	18,9	13,3	9,1	5,7
4800	18,7	12,9	14,3	11,3	6,61	6,5
4900	15,4	10,0	11,9	10,0	3,7	3,0
5000	13,4	9,5	12,1	9,9	4,1	3,2
5100	12,2	9,2	13,4	10,7	4,9	3,9
5200	12,0	9,7	13,7	13,7	5,4	4,3
5300	13,2	10,4	15,9	15,4	6,1	4,5
5400	15,9	11,3	18,0	18,8	6,0	4,5
5500	17,3	11,8	20,6	21,6	5,4	4,4
5600	17,5	12,2	22,8	23,0	5,3	4,3
5700	17,8	12,3	23,4	23,5	5,4	4,2
5800	19,2	12,6	26,6	24,9	5,6	4,4
5900	20,4		30,2	29,3	5,7	4,6
6000	20,9		31,9	32,4	5,6	4,7
6100	21,8	3,0	32,8	34,6	5,4	4,6
6200	21,1		33,3	35,5	5,0	4,3
6300	20,8		33,2	36,4	5,1	4,1
6400	20,4		33,3	36,7	5,2	4,1
6500	19,9		33,2	36,9	5,0	3,9
6600	19,4			37,0		

bution. Apparently, this is to be explained by the enhanced brightness of the sky on that night due to the aurora polaris which was observed visually about 1 hour later /4/.

For the sake of greater clearness, the $I_s(\lambda)$ values quoted in Table 5 are presented in Fig. 3 for all days of observation. An analysis of this Figure leads to the conclusion that the energy distribution in the range of wavelengths 5400 to 4100 A varies slightly from

Table 4

λ	a	b	c	d	e	f	g
4000	4,1	3,8			4,2	6,2	4,0
4200	4,5	4,6	2,3	2,5	5,8	8,4	4,9
4100	4,6	5,0	2,8	3,0	6,0	9,6	5,4
4300	5,2	5,7	3,1	3,2	6,2	10,4	5,9
4400	6,0	6,5	3,4	3,7	7,1	11,4	6,5
4500	6,3	7,1	3,6	3,6	7,4	12,0	6,6
4600	6,1	7,0	3,8	3,9	7,1	11,8	3,7
4700	5,5	6,3	3,5	3,7	6,2	10,4	5,9
4800	5,5	5,9	2,9	3,0	5,6	9,0	5,3
4900	5,2	5,3	2,7	2,8	5,0	8,1	4,6
5000	4,9	4,8	2,5	2,5	4,4	7,2	4,1
5100	4,9	4,8	2,5	2,5	4,3	7,3	4,1
5200	5,2	5,2	2,8	2,8	4,7	7,8	4,6
5300	5,6	6,7	3,1	2,9	5,4	8,5	5,3
5400	6,0	6,5	3,6	3,4	5,8	9,0	5,8
5500	6,7	7,2	3,8	3,5	6,3	10,2	6,2
5600	7,0	7,7	4,4	3,8	6,9	10,8	6,3
5700	7,3	8,5	5,2	4,3	7,5	11,5	6,5
5800	7,7	9,8	5,9	4,8	7,5	12,6	7,2
5900	8,1	11,0	6,6	5,3	8,0	13,6	8,0
6000	8,4	11,7	7,1	5,6	8,4	14,5	8,6
6 00	8,8	12,0	7,6	6,0	8,9	15,5	9,2
6200	9,0	12,0	7,9	6,0	9,0	15,5	9,4
6300	9,1	12,1	8,1	6,2	9,2	15,5	9,4
6400	9,2	12,1	8,3	6,3	9,3	15,6	9,6
6500	9,4	12,1	8,5	7,0	9,6	15,6	9,7

day to day. This is possibly caused by variations in the intensity of the molecular bands. These bands virtually coincide with the continuous spectrum, but on some days they stand out against it.

The results obtained for the energy distribution in the range of 5400 – 6500 A are not entirely reliable, because the wings of the emission lines 5577, 5893 and 6300 overlap due to the small dispersion of the spectograph. For this reason, the $I_s(\lambda)$ values could only be obtained for the wavelengths 6 500, 6 100, 5 700 and 5450 A, in

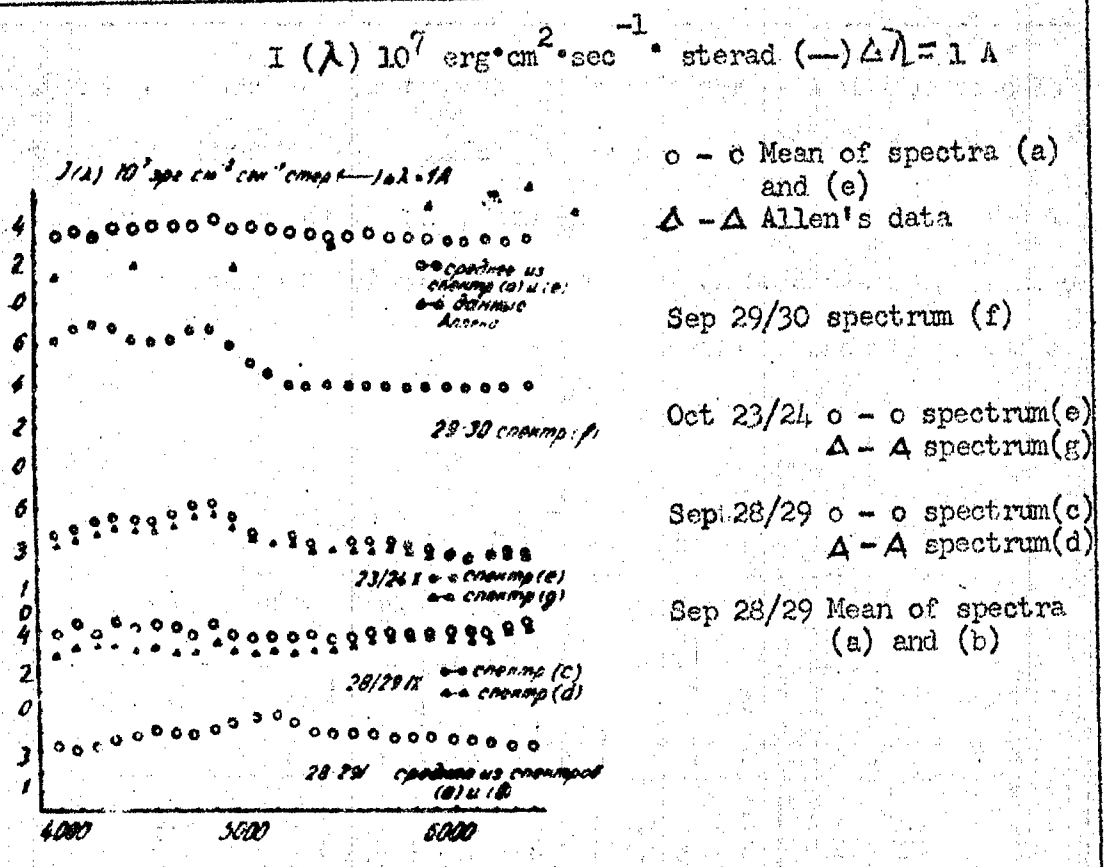

Fig. 3

respect to which allowance was made for the instrumental contour ascertained by special investigations. The $I_s(\lambda)$ values for the intermediate wavelengths were determined by interpolation.

Allen's points (triangularly shaped) have been plotted on the graph in Fig. 4 for purposes of comparison. As is seen, they deviate considerably from our own data with respect to both absolute values and energy distribution in the spectra.

We also determined, for all 7 spectrograms, the integral brightnesses of the emission lines of the night sky in absolute units, i.e., in erg/cm^2·sec·sterad. The results are set forth in Table 6 as

follows: column 1 — serial number of spectra, columns 2, 3, and 4 — intensity values of emission lines, column 5 — integral brightness of the continuous spectrum of the night sky in the wavelength range between 4100 and 6500 A, and column 6 — ratio of emission components to the continuous spectrum.

Table 5

λ	Circumpolar region					Region around β *Dra*		Mean for pole
	27/28.IX		28/29.IX		23/24 X	29/30 IX	23/24 X	
	a	*b*	*c*	*d*	*e*	*f*	*g*	*h*
1	2	3	4	5	6	7	8	9
4100	3,1	3,1	2,7	3,8	3,7	6,1	3,2	3,3
4200	2,9	3,1	3,1	4,3	4,0	6,8	3,6	3,5
4300	3,0	3,3	3,2	3,8	4,1	7,0	3,9	3,3
4400	3,3	3,6	3,2	4,3	4,5	6,8	4,2	3,8
4500	3,5	3,9	3,0	4,0	4,2	6,4	3,9	3,7
4600	3,5	4,0	3,2	4,2	4,2	6,2	3,9	3,8
4700	3,5	4,0	2,9	4,0	4,4	6,3	4,2	3,8
4800	3,7	4,0	2,9	3,7	5,0	6,9	4,7	3,8
4900	4,0	4,1	3,4	4,3	5,1	7,0	4,7	4,2
5000	4,3	4,3	2,9	3,8	4,5	6,1	4,1	3,8
5100	4,6	4,5	2,8	3,5	3,8	5,2	3,6	3,8
5200	4,7	4,6	3,0	3,7	3,3	4,7	3,2	3,7
5300	4,3	4,4	2,8	3,6	3,4	4,3	3,3	3,7
5400	3,7	4,0	3,0	3,7	3,1	4,2	3,0	3,5
5500	3,6	3,9	3,0	3,4	3,0	4,2	3,0	3,4
5600	3,6	3,9	3,2	3,5	3,2	4,2	2,9	3,5
5700	3,5	4,1	3,5	3,7	3,2	4,2	2,9	3,6
5800	3,2	4,1	3,5	3,6	3,2	4,1	3,0	3,5
5900	3,1	4,2	3,6	3,6	3,0	4,1	2,9	3,5
6000	3,1	4,2	3,8	3,6	2,7	4,1	2,8	3,5
6100	3,0	4,0	3,7	3,4	2,6	4,1	2,7	3,3
6200	2,9	3,9	3,8	3,3	2,6	4,1	2,7	3,3
6300	2,9	3,8	3,7	3,3	2,6	4,1	2,6	3,4
6400	2,8	3,7	3,9	3,8	2,6	4,1	2,7	3,4
6500	2,8	3,6	4,0	4,2	2,6	4,0	2,7	3,4

Table 6

Spectrum	5577	5894	6300 + 6364	$\Sigma I_s(\lambda)$ $\lambda=6500$ / $\lambda=4100$	$\Sigma I_{emission} / \Sigma I_s(\lambda)$
1	2	3	4	5	6
a	$12,4 \cdot 10^{-5}$	$5,6 \cdot 10^{-5}$	$10,3 \cdot 10^{-5}$	$86,4 \cdot 10^{-5}$	0,33
b	13,9	6,7	4,5	98,6	0,26
c	12,4	8,4	7,1	78,4	0,36
d	17,8	5,6	4,9	92,1	0,31
e	31,2	10,5	15,5	87,3	0,65
f	31,2	8,1	19,9	131,0	0,45
g	32,4	9,1	17.0	82,3	0,71

A description of the spectrograms is furnished in Table 7 (columns 1 - 5) as follows: 1 — designation of spectrum, 2 — dates, 3 — universal time at the middle of exposure, and 5 — stars used for standardization.

Table 7

Spectrum	Dates	*U.T.*	Region of sky	Remarks
1	2	3	4	5
a	27/28.IX	15^h04^m	Pole	8 *Cyg*
b	27/28	19 25	"	" " "
c	28/29	18 00	"	*a Lyr* and luminophor
d	28/29	21 38	"	" "
e	23/24.X	15 50	"	β *Dra* " "
f	29/30.IX	16 36	β *Dra*	" "
g	23/24.X	15 06	"	" "

As may be seen from Table 6, the ratio of the integral brightness of the continuous spectrum to the total brightness of the emission lines varies appreciably from one day to the other. This is a conse-

quence of fluctuations in brightness of the emission lines themselves which may change within a range of 200-300 per cent. On an average, $\frac{I_{emission}}{I_s(\lambda)} = 0.44$, which means that the continuous spectrum provides about 40 % of the total brightness of the nocturnal sky. However, actually this value is somewhat overestimated due to the fact that the emission bands in the blue part of the spectrum (4800 - 4000 A) are not resolved in a nephelometric spectrograph. To arrive at a reliable estimate of the share of the continuous spectrum in this region, the observations should be carried out with an instrument having a wider range of dispersion.

In conclusion, the authors feel obliged to express their thanks to Acad. V. G. Fesenkov, who suggested the subject of this study, to N. N. Pariyskiy and L. M. Gindilis for their assistance during the observations and for placing at our disposal data on the energy distribution in the spectrum of the luminophor.

References

1. C. W. Allen: Astrophysical Quantities, London, p. 125 (1955).
2. H. W. Babcock and J. J. Johnson: — Ap. J., 94, 271 (1941).
3. K. K. Chuvayev: Izv. Krym. Astr. Obs.(News of the Crimean Astron. Observ.) 1953, vol. X, 54.
4. Z. V. Karyagina : Izv. Astrofiz. In-ta A N KazSSR (News of the Astrophys. Inst., Ac. Sci. Kazakh SSR) 1959, vol. VIII, 68.

5. N. N. Pariyskiy, L. M. Gindilis: ASh (Astron.Journal), vol. XXXVI, ed. 3, 539, 1950.

6. Ann. Aph. Obs. Smithonian Inst., vol. V, 165, 1950.

7. A. Unsold : Fizika Zvezdnykh Atmosfer(Physics of Stellar Atmospheres), Moscow, 41, 1949.

8. Brill: A. N., 223, 106 (1925).

9. H. Kienle, H. Strassl, J. Wempe, Zt. f. Aph. 16, ed.4,201(1938)

10. Z. V. Karyagina : Izv. Astrofiz. In-ta A N KazSSR, 1953, vol. 1, ed. 1-2.

11. O. Eggen, A.J., 60, 65, 1955.

ON THE COLOR OF THE TWILIGHT SKY AT ZENITH

Pp 96 - 107 by N. B. Divari

In 1938 Grandmontagne /1/ detected differences in the curve of brightness variation of the twilight sky at zenith for blue and red rays. His observations, which covered submergences of the Sun exceeding 5°, showed that in red rays the twilight at zenith terminates by 3° earlier than in blue rays. Yet the spectrophotometric observations carried out in the same year by dufay and Gauzit /2/ did not reveal any difference in the zenithal twilight intensities depending on wavelength. The authors found that in the range of solar submergences between 5 and 8° 30' the energy distribution in the twilight spectrum remains virtually unchanged, in other words, the brightness curves plotted as a function of solar submergence for the different wavelengths run parallel to each other. These findings were, however, disproved by later research. Thus, in 1946 T. G. Megrelishvili /3/ discovered that the brightness ratio of the twilight sky in blue and red rays varies, first rising up to an angle of submergence of the Sun of 10° and falling off thereafter. A like correlation was established by observations carried out on the Kamenskoye plateau in 1955. According to Sidentopf's data, cited by Bullrich /5/ and Ashburn /6/, the color temperature scale of the radiation of the twilight sky varies from

6500 to 17900°K, culminating at a submergence angle of 10°. Ashburn's measurements /7/, relating to the spectral region between 440 and 750 mμ, disclosed that the energy distribution in the visible part of the spectrum reaches its minimum intensity near λ = 540 mμ and, further, that the color of the twilight sky changes very appreciably with the degree of submergence of the Sun. Gadsden /8/, who performed observations in London in 1956, determined the chromaticity of the twilight sky under the international colorimetric system and compared his results with the computed values. It appeared that the coloration of the sky depends on ozone absorption of solar radiation, which is in accord with the theoretical results of Hulbart /9/, who established a strong influence of the presence of ozone on the color of the twilight sky.

In the Fall of 1956, we conducted observations of the zenithal twilight radiation with the aid of an electrophotometer designed by V. I. Moroz /10/ and interference light filters centered to these wavelengths: 367; 369; 405; 437; 554; 580 and 593 mμ. The transmission curves for the filters used, taking into account the sensitivity of the radiation receiver (an FEU-19M photomultiplier), are shown in Fig. 1. Table 1 gives the basic features of each filter.

The observations were carried out on the Kamenskoye plateau (φ = 43°.2 N, λ = 76° 56' E; H = 1450 m above s.l.) during the period Oct 9 to Nov 1, 1956. The measuring results for the twilight sky were expressed in absolute units, viz., in erg/cm^2·sec·A per 1 sq.

degree, by tying the values obtained to star brightness with reduction to class G star intensity. The transparency factor needed for the tie

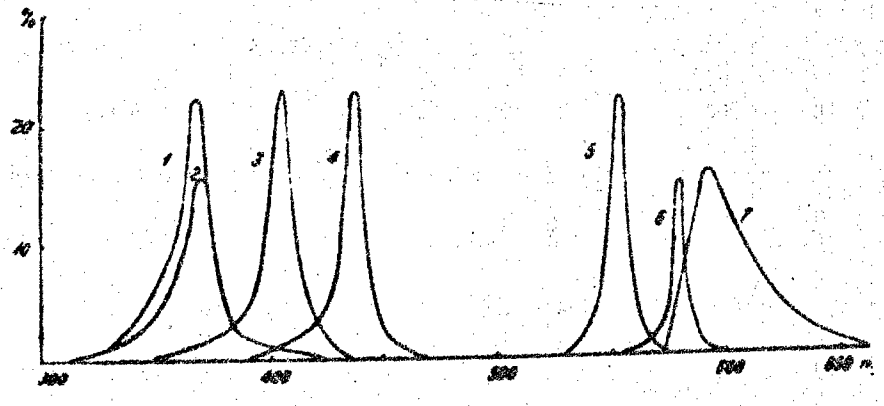

Fig. 1. Transmission curves of filters (photomultiplier sensitivity considered).

was determined on data obtained by N. I. Ovchinnikova (from observations of the Sun with a halo-photometer) and V. S. Matyagin (from photographic observations of stars). In Table 2 are given the observed

T a b l e 1

Basic features of filters used

No. of filter	Position Of maximum transmissivity	Transmissivity at maximum, %	Half-width of band-pass	Remarks
				Interference filter
1	367	22	160 A	
2	369	16	140	
3	405	23	110	
4	437	23	90	
5	554	22	80	
6	580	15	60	
7	593	16	310	Glass filter

Table 2

Mean values of observed zenithal brightnesses of the twilight sky in different rays
(In erg/cm^2·sec.A per 1 sq.°)

$g_\odot$	№ 1 λ=367 mμ	№ 2 λ=369 mμ	№ 3 λ=405 mμ	№ 4 λ=437 mμ
0°	$7,3\cdot10^{-5}$	$8,0\cdot10^{-5}$		
1	$4,2\cdot10^{-5}$	$5,2\cdot10^{-5}$		
2	$2,5\cdot10^{-5}$	$2,8\cdot10^{-5}$	$2,1\cdot10^{-5}$	$2,2\cdot10^{-5}$
3	$1,1\cdot10^{-5}$	$1,2\cdot10^{-5}$	$1,0\cdot10^{-5}$	$1,1\cdot10^{-5}$
4	$4,0\cdot10^{-6}$	$4,3\cdot10^{-6}$	$3,4\cdot10^{-6}$	$3,6\cdot10^{-6}$
5	$1,4\cdot10^{-6}$	$1,5\cdot10^{-6}$	$1,1\cdot10^{-6}$	$1,2\cdot10^{-6}$
6	$4,3\cdot10^{-7}$	$4,6\cdot10^{-7}$	$3,6\cdot10^{-7}$	$3,8\cdot10^{-7}$
7	$1,3\cdot10^{-7}$	$1,4\cdot10^{-7}$	$1,0\cdot10^{-7}$	$1,1\cdot10^{-7}$
8	$4,2\cdot10^{-8}$	$4,6\cdot10^{-8}$	$3,4\cdot10^{-8}$	$3,5\cdot10^{-8}$
9	$1,5\cdot10^{-8}$	$1,6\cdot10^{-8}$	$1,2\cdot10^{-8}$	$1,2\cdot10^{-8}$
10	$6,3\cdot10^{-9}$	$6,7\cdot10^{-9}$	$4,9\cdot10^{-9}$	$6,7\cdot10^{-9}$
11	$2,8\cdot10^{-9}$	$3,1\cdot10^{-9}$	$2,2\cdot10^{-9}$	$2,2\cdot10^{-9}$
12	$1,5\cdot10^{-9}$	$1,3\cdot10^{-9}$	$9,6\cdot10^{-10}$	$9,8\cdot10^{-10}$
13	$5,4\cdot10^{-10}$	$5,8\cdot10^{-10}$	$4,3\cdot10^{-10}$	$4,4\cdot10^{-10}$
14	$3,1\cdot10^{-10}$	$3,2\cdot10^{-10}$	$2,4\cdot10^{-10}$	$2,6\cdot10^{-10}$
15	$2,2\cdot10^{-10}$	$2,4\cdot10^{-10}$	$1,8\cdot10^{-10}$	$1,8\cdot10^{-10}$
16	$1,8\cdot10^{-10}$	$1,9\cdot10^{-10}$	$1,3\cdot10^{-10}$	$1,5\cdot10^{-10}$
17	$1,6\cdot10^{-10}$	$1,7\cdot10^{-10}$	$1,2\cdot10^{-10}$	$1,4\cdot10^{-10}$
18°	$1,6\cdot10^{-10}$	$1,7\cdot10^{-10}$	$1,0\cdot10^{-10}$	$1,2\cdot10^{-10}$

$g_\odot$	№ 5 λ=554 mμ	№ 6 λ=580 mμ	№ 7 λ=593 mμ
0°	$1,7\cdot10^{-5}$	$3,1\cdot10^{-5}$	
1	$1,7\cdot10^{-5}$	$1,9\cdot10^{-5}$	$1,6\cdot10^{-5}$
2	$1,2\cdot10^{-5}$	$1,0\cdot10^{-5}$	$1,0\cdot10^{-5}$
3	$5,6\cdot10^{-6}$	$4,5\cdot10^{-6}$	$4,1\cdot10^{-6}$
4	$1,6\cdot10^{-6}$	$1,2\cdot10^{-6}$	$1,2\cdot10^{-6}$
5	$5,2\cdot10^{-7}$	$3,7\cdot10^{-7}$	$3,7\cdot10^{-7}$
6	$1,5\cdot10^{-7}$	$1,1\cdot10^{-7}$	$1,1\cdot10^{-7}$
7	$4,4\cdot10^{-8}$	$3,1\cdot10^{-8}$	$2,8\cdot10^{-8}$
8	$4,4\cdot10^{-8}$	$9,5\cdot10^{-9}$	$9,9\cdot10^{-9}$
9	$4,6\cdot10^{-9}$	$3,1\cdot10^{-9}$	$2,8\cdot10^{-9}$
10	$1,8\cdot10^{-9}$	$1,2\cdot10^{-9}$	$1,2\cdot10^{-9}$
11	$9,0\cdot10^{-10}$	$5,8\cdot10^{-10}$	$5,9\cdot10^{-10}$
12	$4,8\cdot10^{-10}$	$3,1\cdot10^{-10}$	$3,2\cdot10^{-10}$
13	$3,1\cdot10^{-10}$	$2,1\cdot10^{-10}$	$2,2\cdot10^{-10}$
14	$2,4\cdot10^{-10}$	$1,8\cdot10^{-10}$	$1,8\cdot10^{-10}$
15	$2,4\cdot10^{-10}$	$1,6\cdot10^{-10}$	$1,8\cdot10^{-10}$
16	$2,1\cdot10^{-10}$	$1,6\cdot10^{-10}$	$1,7\cdot10^{-10}$
17	$2,3\cdot10^{-10}$	$1,7\cdot10^{-10}$	$1,7\cdot10^{-10}$
18°	$2,7\cdot10^{-10}$	$1,7\cdot10^{-10}$	$1,6\cdot10^{-10}$

brightness values of the twilight sky for different filters, by steps of one degree of arc, averaged from observations made on October 9, 12, 13, 14, 29, 30, 31 and November 1.

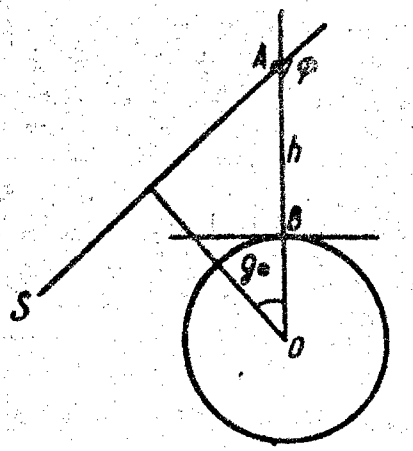

Fig. 2. Schematic diagram of movement of rays for computing the intensities of twilight luminescence (first-order scattering)

With a view to evaluating the results obtained, we computed the intensities of the solar emission scattered by the Earth's atmosphere at dusk for selected wavelengths. The computations were carried out taking into account radiation scattering of the first order for the spherical atmosphere, with a density distribution as given in /11/ and making no allowance for refraction and the apparent size of the solar disk.

The absorption of solar radiation by pure air along the path S A (Fig. 2.) is determined by the optical thickness x.

$$x = \frac{1}{n(0)} \int n(h)\, ds, \qquad (1)$$

where $n(h)$ is the number of particles per unit volume at the height h above the Earth's surface, and $n(0)$ is the number of particles at sea level under normal conditions/atmospheric. Due to absorption by pure air, the monochromatic solar radiation of the intensity I_0 is attenuated at the point A to the value $I_0 e^{-\beta x}$, where β is the absorption coefficient of pure air, whose values were taken from Van de Holst's work /12/. The absorption by ozone along the same path $S\,A$ is taken account of by the factor $e^{-\alpha x_1}$, where α is the absorption coefficient of ozone calculated per 1 cm of the reduced ozone thickness; x_1 is the reduced thickness of the layer of ozone on the path $S\,A$ and is equal to

$$x_1 = \int m(h)\, ds, \tag{2}$$

where $m(h)$ is the ozone concentration at the height h.

Hence, at the point A the solar radiation intensity equals $I_0 e^{-\beta x} e^{-\alpha x_1}$. Taking the Rayleigh indicatrix of scattering in the direction toward the observer at B, the energy dissipated by a unit volume dv inside the solid angle $d\omega'$ is equal to

$$I_0 e^{-\beta x} e^{-\alpha x_1} \sigma (1 + \cos^2 \varphi) \rho_H \, d\omega' \, dv, \tag{3}$$

where ρ_H is the air density at the height h, and σ is the scattering factor which is related to the absorption coefficient by the ratio $\sigma = \frac{1}{4\pi} \beta$ (the depolarization factor being taken as equal to zero). The light absorption on the path $A\,B$ is determined by the factor $e^{-\tau_H}$, where

$$\tau_H = \frac{\beta}{n(0)} \int n(h)\, dh. \tag{4}$$

Substituting in Expression (3) the equivalent of $dv = h^2 d\omega dh$ (where $d\omega$ is the solid angle at which the unit dv is seen at the height h above the Earth's surface), dividing by $h^2 d\omega$ and integrating over h, we get the following Expression for the brightness of the sky, B:

$$B = I_0 \sigma (1 + \cos^2 \varphi) d\omega \int_0^\infty \rho_h e^{-\beta x - \alpha x_1 - \tau_h} dh . \qquad (5)$$

The integrals (1), (2), (3), (4), (5) were taken by the method of numerical integration. To this end, the atmosphere was divided into concentric layers of the following thicknesses: 1 km (height 0 to 10 km); 5 km (height 10 to 40 km); 10 km (height 40 to 150 km); and 50 km (h = 150 km and over). The values for the absorption coefficient of ozone α were taken from ref. /13/ after reducing same to the basis of e, and the ozone distribution with respect to altitude, from data reported by Johnson and co-workers in ref. /14/. For altitudes below 20 km the ozone distribution was taken according to A. Kh. Khrgian's data cited in ref. /13/.

In Table 3 are presented brightness values, calculated from Formula (5), of the twilight sky for different wavelengths and different submergences of the Sun without allowing for ozone absorption; in Tables 4 and 5 similar data are given, allowance being made for absorption by ozone at a total content of the latter of 0.212 and 0.400 cm, respectively.

Table 3

Calculated brightness values of the twilight sky in erg/cm^2·sec·A per 1 sq. degree (without allowing for ozone absorption)

$z_\odot$	λ=0,37 μ	λ=0,44 μ	λ=0,50 μ	λ=0,55 μ	λ=0,58 μ
0°	$2{,}9\cdot10^{-5}$	$7{,}5\cdot10^{-5}$	$1{,}0\cdot10^{-4}$	$1{,}06\cdot10^{-4}$	$1{,}06\cdot10^{-4}$
2	$1{,}1\cdot10^{-5}$	$2{,}4\cdot10^{-5}$	$3{,}1\cdot10^{-5}$	$3{,}3\cdot10^{-5}$	$3{,}3\cdot10^{-5}$
4	$1{,}6\cdot10^{-6}$	$3{,}8\cdot10^{-6}$	$4{,}7\cdot10^{-6}$	$4{,}8\cdot10^{-6}$	$5{,}0\cdot10^{-6}$
6	$1{,}6\cdot10^{-7}$	$3{,}3\cdot10^{-7}$	$3{,}6\cdot10^{-7}$	$3{,}4\cdot10^{-7}$	$3{,}3\cdot10^{-7}$
8		$5{,}5\cdot10^{-9}$		$7{,}9\cdot10^{-9}$	$8{,}3\cdot10^{-9}$
10	$2{,}7\cdot10^{-11}$	$4{,}5\cdot10^{-11}$	$4{,}6\cdot10^{-11}$	$4{,}2\cdot10^{-11}$	$4{,}0\cdot10^{-11}$
12	$2{,}8\cdot10^{-12}$				
14	$2{,}5\cdot10^{-13}$	$3{,}1\cdot10^{-13}$	$2{,}5\cdot10^{-13}$	$1{,}8\cdot10^{-13}$	$1{,}5\cdot10^{-13}$
18°	$1{,}5\cdot10^{-14}$	$1{,}9\cdot10^{-14}$	$1{,}5\cdot10^{-14}$	$1{,}1\cdot10^{-14}$	$8{,}4\cdot10^{-15}$

$z_\odot$	λ=0,60 μ	λ=0,65 μ	λ=0,70 μ
0°	$1{,}04\cdot10^{-4}$	$9{,}7\cdot10^{-5}$	$7{,}4\cdot10^{-5}$
2	$3{,}4\cdot10^{-5}$	$3{,}4\cdot10^{-5}$	$2{,}9\cdot10^{-5}$
4	$5{,}0\cdot10^{-6}$	$5{,}1\cdot10^{-6}$	$4{,}6\cdot10^{-6}$
6	$3{,}2\cdot10^{-7}$	$3{,}1\cdot10^{-7}$	$2{,}5\cdot10^{-7}$
8			
10	$4{,}3\cdot10^{-11}$	$3{,}9\cdot10^{-11}$	$3{,}2\cdot10^{-11}$
12			
14	$1{,}3\cdot10^{-13}$	$9{,}8\cdot10^{-14}$	$6{,}5\cdot10^{-14}$
18°	$7{,}4\cdot10^{-15}$	$5{,}3\cdot10^{-15}$	$3{,}4\cdot10^{-15}$

Table 4

Calculated brightness values of the twilight sky in erg/cm^2·sec. A per 1 sq. degree (allowance made for ozone absorption) at a total ozone content of 0.212 cm

$g_\odot$	λ=0,50 μ	λ=0,55 μ	λ=0,58 μ	λ=0,60 μ	λ=0,70 μ
0°	$8{,}9\cdot10^{-5}$	$7{,}6\cdot10^{-5}$	$6{,}6\cdot10^{-5}$	$6{,}2\cdot10^{-5}$	$6{,}9\cdot10^{-5}$
2	$2{,}6\cdot10^{-5}$	$2{,}1\cdot10^{-5}$	$1{,}8\cdot10^{-5}$	$1{,}8\cdot10^{-5}$	$2{,}6\cdot10^{-5}$
4	$3{,}7\cdot10^{-6}$	$2{,}6\cdot10^{-6}$	$2{,}3\cdot10^{-6}$	$2{,}2\cdot10^{-6}$	$4{,}1\cdot10^{-6}$
6	$2{,}9\cdot10^{-7}$	$1{,}8\cdot10^{-7}$	$1{,}3\cdot10^{-7}$	$1{,}2\cdot10^{-7}$	$2{,}1\cdot10^{-7}$
8		$3{,}9\cdot10^{-9}$	$3{,}1\cdot10^{-9}$		
10	$3{,}8\cdot10^{-11}$	$2{,}4\cdot10^{-11}$	$1{,}9\cdot10^{-11}$	$1{,}8\cdot10^{-11}$	$2{,}7\cdot10^{-11}$
14		$1{,}4\cdot10^{-13}$	$1{,}1\cdot10^{-13}$	$9{,}3\cdot10^{-14}$	$6{,}0\cdot10^{-14}$
18°		$9{,}0\cdot10^{-15}$	$6{,}7\cdot10^{-15}$	$5{,}8\cdot10^{-15}$	$3{,}2\cdot10^{-15}$

Table 5

Calculated brightness values of the twilight sky in erg/cm^2·sec. A per 1 sq. degree (allowance made for ozone absorption) at a total ozone content of 0.400 cm

$g_\odot$	λ=0,50 μ	λ=0,55 μ	λ=0,58 μ	λ=0,60 μ	λ=0,65 μ	λ=0,70 μ
0°	$8{,}0\cdot10^{-5}$	$5{,}6\cdot10^{-5}$	$4{,}4\cdot10^{-5}$	$4{,}0\cdot10^{-5}$	$6{,}3\cdot10^{-5}$	$6{,}4\cdot10^{-5}$
2	$2{,}2\cdot10^{-5}$	$1{,}4\cdot10^{-5}$	$1{,}1\cdot10^{-5}$	$1{,}0\cdot10^{-5}$	$2{,}0\cdot10^{-5}$	$2{,}4\cdot10^{-5}$
4	$3{,}1\cdot10^{-6}$	$1{,}7\cdot10^{-6}$	$1{,}1\cdot10^{-6}$	$1{,}1\cdot10^{-6}$	$2{,}6\cdot10^{-6}$	$3{,}6\cdot10^{-6}$
6	$2{,}3\cdot10^{-7}$	$1{,}1\cdot10^{-7}$	$5{,}6\cdot10^{-8}$	$5{,}8\cdot10^{-8}$	$1{,}3\cdot10^{-7}$	$1{,}8\cdot10^{-7}$
8		$2{,}1\cdot10^{-9}$	$1{,}4\cdot10^{-9}$			
10		$1{,}7\cdot10^{-11}$	$1{,}1\cdot10^{-11}$	$1{,}0\cdot10^{-11}$		
14		$1{,}3\cdot10^{-13}$	$9{,}2\cdot10^{-14}$	$8{,}0\cdot10^{-14}$		
16°		$8{,}1\cdot10^{-15}$	$6{,}0\cdot10^{-15}$	$5{,}2\cdot10^{-15}$		

Comparison of the calculated and observed brightness values brings out the fact that the intensity of the observed twilight luminescence for all wavelengths of the visible part of the spectrum is fairly close to the intensity of scattered radiation of the first order in the range of solar submergence between 0° and $6^{\circ}.5$ only.

At greater submergences the observed intensities, as is seen from Figs. 3,4,5 and 6, are by several orders higher than the computed scattering intensities of the first order. This result is in accord with Hulbart's results /9/, who made a comparison of the computed brightness with the values obtained by observations on the peak of Sacramento.

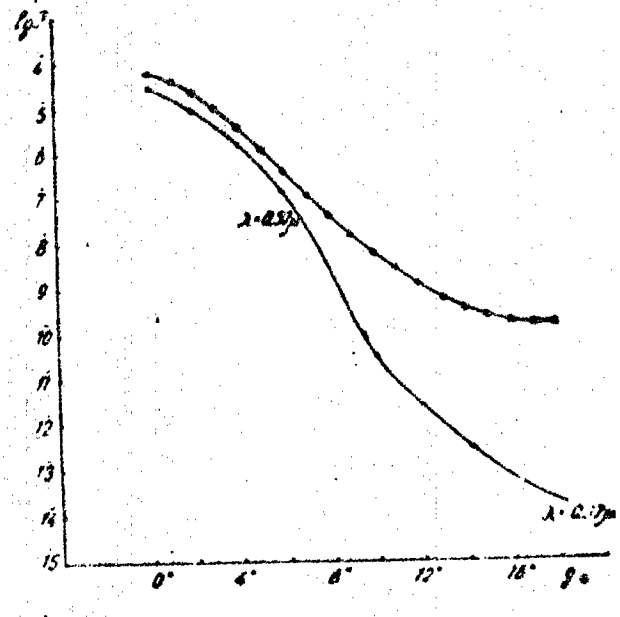

Fig. 3. Comparison of observed brightnesses (crosslets) of the twilight sky for $\lambda = 0.37\mu$ with the computed values (scattering of the first order).

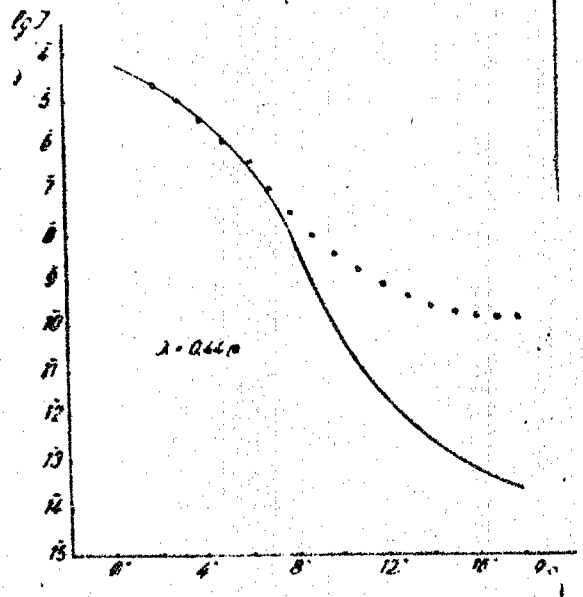

Fig. 4. Comparison of observed brightnesses (crosslets) of the twilight sky for $\lambda = 0.44\mu$ with the computed values (scattering of the first order).

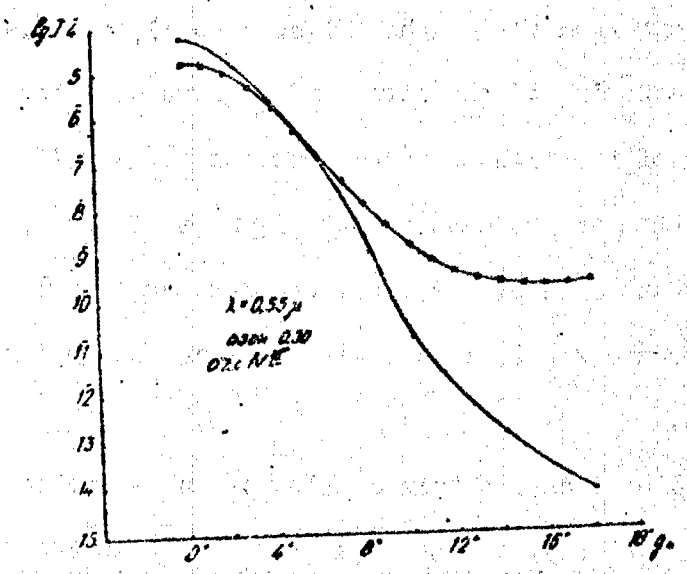

Fig. 5. Comparison of observed brightness (crosslets of the twilight sky for = 0.55 with computed values (scattering of the first order at 0.30 cm ozone).

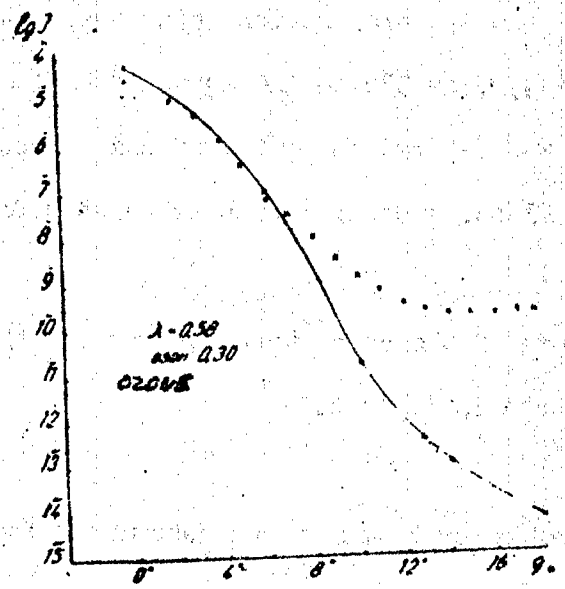

Fig. 6. Comparison of observed brightness (crosslets of the twilight sky for = 0.58 with computed values (scattering of the first order at 0.30 cm ozone).

As is apparent from the graphs (Figs. 3 to 6), at $8^{\circ}.5$ and up, counting only scattering of the first order gives brightness values even below those of the nightsky (at submergences $g_{\odot} = 18^{\circ}$.) It can thus be assumed that in the case of submergences of the Sun exceeding $8^{\circ}.5$ radiation scattering of the first order plays a negligibly small part in the aggregate zenithal radiative flux in all regions of the visible spectrum.

The observational data obtained allow of an estimation as to the color of the twilight sky, taking as a characteristic the color temperature, as was also done by Sidentopf /5,6/. As was to be expected, the observed energy distribution in the investigated region of the spectrum cannot be represented by the temperature value alone. Therefore, the spectral region under observation was divided into two parts, viz., from 370 to 440 mμ and from 440 to 600 mμ. The color temperature was determined by way of comparison of the observed distribution with Planck's distribution calculated for several temperatures.

The mean values of the color temperatures for the two spectral regions are set forth in Table 6.

Table 6

Mean values of color temperatures determined from Planck's curves

$g_{\odot}$	2°	3°	4°	5°	6°	7°	8°	9°	10°	11°	12°	13°	14°	15°	16°
Region 370–440 mμ	11	11	11	11	11	12	13	12	13	13	12	12	12	14	14
Region 440–600 mμ	9	10	16	21	24	24	27	34	37	31	17	9	7	6	5

As is seen from the tabulated data, the color temperature for the spectral region 440 to 600 mμ varies as a function of the Suns's submergence below the horizon, reaching its maximum value at a submergence of about 10°. In the blue part of the spectrum (in the interval of 370 to 440 mμ) these variations are almost competely absent. It can accordingly be assumed that the region between 440 and 600 mμ is mainly responsible for changes in the coloration of the twilight sky; this interval, indeed, is identical with Chappuis' band - the region of ozone absorption. This conclusion is substantiated by a comparison of the observed energy distribution with the corresponding theoretical values.

Plotted on the graphs in Fig. 7 are the curves of energy distribution in the spectrum of the twilight sky for submergences of 0°, 2°, 4° and 6°, so computed as to take account solely of first-order scattering for the pure atmosphere (upper curves). Also shown are distribution curves obtained when allowing for the presence of ozone estimated at 0,212 cm (middle curves) and 0.400 cm (lower curves). The observed brightness values are marked with crosslets. As will be noted from the graphs, the observed energy distribution is in a very great measure accounted for by ozone absorption in the Chappuis band.

At solar submergences of 2° and 4° it proved closest to the distribution corresponding to a total ozone content of 4 mm. At submergences exceeding 6° the observed brightness values, as mentioned above, cannot be represented by values computed with scattering of the first

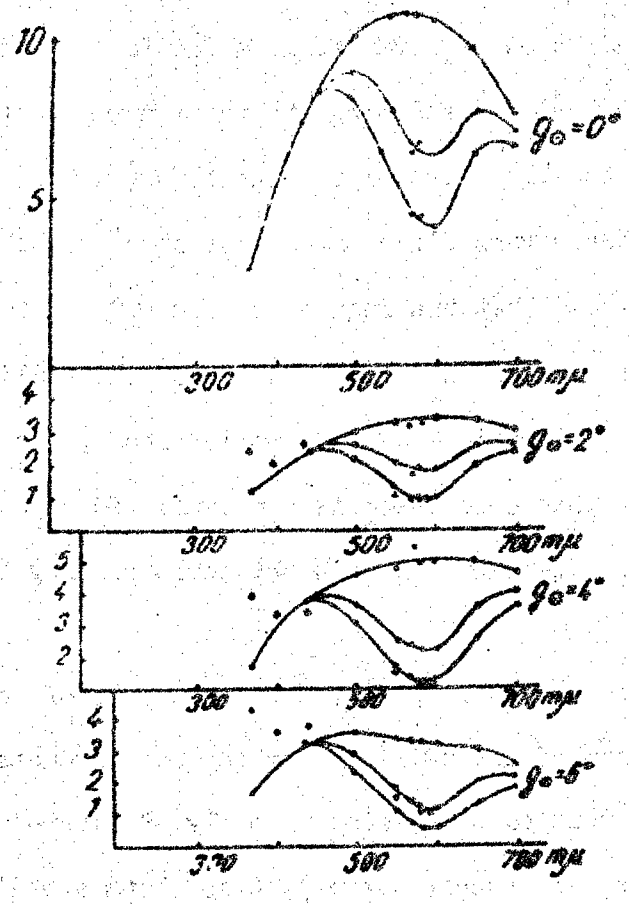

Fig. 7. Energy distribution in the spectrum of the twilight sky at different degrees of solar submergence. Crosslets denote observed values, points- values calculated for scattering of the first order at different ozone contents indicated in the text.

order alone being taken into account. For this reason, the observed brightnesses corresponding to the energy distribution curves are found to be considerably in excess of the theoretical values.

The ratio of the radiation intensities in two spectral regions may serve as another characteristic of the color of the twilight sky. Table 7 gives the values for the observed brightness ratios in two re-

gions of the spectrum. As is apparent from the data in this Table, in the blue part of the spectrum ($\lambda < 440$ mμ) these ratios vary inappreciably (second and third columns) as compared with the intensity ratios of the blue part of the spectrum to Chappuis' band (3rd, 4th and 5th columns). This entirely agrees with the result obtained above in the discussion of the color temperatures.

In order to define more accurately the reasons for the different course of the radiation-intensity ratio in the blue and yellow-green parts of the spectrum, it is interesting to compare the observed values for these ratios with the computed ones. Figs. 8 and 9 show the calculated smoothed curves for the ratios I_{440}/I_{550} and I_{440}/I_{580} for pure air (lower curves) and the ozonous atmosphere containing a total of 0.212 cm (second curves from bottom), 0.300 cm (third curves from bottom) and 0.400 cm (upper curves).

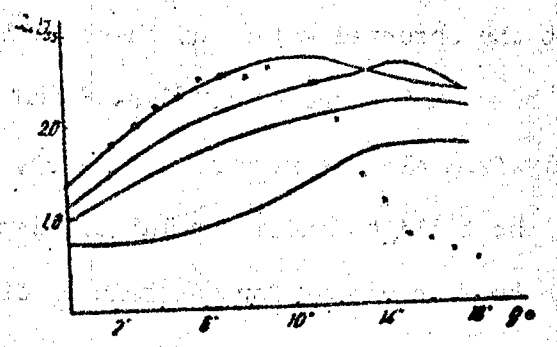

Fig. 8. Comparison of observed I_{440}/I_{550} ratios (crosslets) with the computed values for scattering of the first order at different ozone contents indicated in the text.

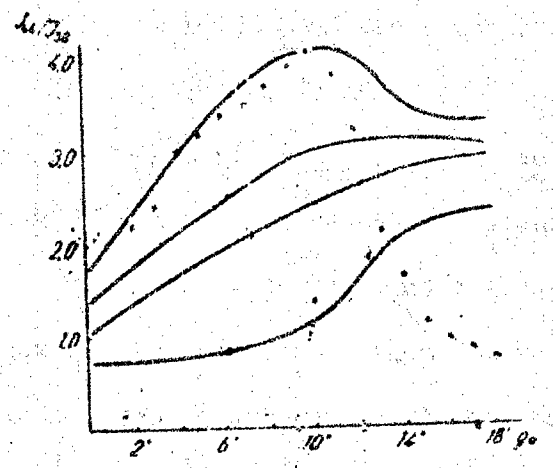

Fig. 9. Comparison of observed I_{440}/I_{580} ratios (crosslets) with the computed values for scattering of the first order at different ozone contents indicated in the text.

As seen from the graphs, the observed trend of the ratios I_{437}/I_{554} (marked with crosslets) corresponds best to the ozone content of 0.400 cm, which accords with the results plotted on the graphs in Fig. 7. (Note that the observed values of these ratios for the case $g_{\odot} = 10°$ are not shown on the graphs of Figs. 8 and 9 because they diverge very strongly from all the remaining values). The described intensity ratios of the twilight radiation largely depend on the ozone content, which can be made use of for determining its proportion in the terrestrial atmosphere at dusk. However, the observed trend of the brightness ratios of the twilight sky only agrees with the computed values at solar submergences up to 8 - 9°. Above this mark, the observed values are less than the theoretical ones.

This shows that at like degrees of submergence twilight comes to an end at zenith and a transitional period begins that leads over to night-time. The sharp fall in the observed values of the ratios concerned in the case of large submergences of the Sun is due to the fact that at night the radiation intensity in the yellow-green part of the spectrum prevails over that of the blue part. In conditions of early twilight, the opposite picture is observed in that the intensity of the blue rays exceeds that of the red ones. We have to conclude from this that twilight at zenith ends at about 8 to 9°. The interval from 9° to 14°

Table 7

Observed values of the intensity ratios of two different spectral regions of the twilight sky

$g_{\odot}$	I_{361}/I_{404}	I_{367}/I_{427}	I_{427}/I_{534}	I_{427}/I_{580}	I_{427}/I_{593}
2°	1,2	1,1	1,8	2,2	2,2
3	1,1	1,0	2,0	2,4	2,7
4	1,2	1,1	2,2	3,0	3,0
5	1,3	1,2	2,3	3,2	3,2
6	1,2	1,1	2,5	3,4	3,4
7	1,3	1,2	2,5	3,5	3,9
8	1,2	1,2	2,5	3,7	3,5
9	1,2	1,2	2,6	3,9	4,3
10	1,3	0,93	3,7	5,6	5,6
11	1,3	1,3	2,4	3,8	3,7
12	1,6	1,5	2,0	3,2	3,1
13	1,3	1,2	1,4	2,1	2,0
14	1,3	1,2	1,1	1,6	1,4
15	1,2	1,2	0,75	1,1	1,0
16	1,4	1,2	0,71	0,94	0,88
17	1,3	1,1	0,61	0,82	0,82
18°	1,6	1,3	0,44	0,70	0,75

may be regarded as intermediate between twilight and night. At over

Table 8

Altitudes of effective twilight ray at different angles of submergence (in km)

$g_\odot$	$\lambda=0,37\ \mu$	$\lambda=0,40\ \mu$	$\lambda=0,44\ \mu$	$\lambda=0,50\ \mu$	$\lambda=0,55\ \mu$
0°	25	22	18	14	12
1	29	25	22	18	16
2	32	29	25	22	20
3	39	36	32	28	25
4	45	42	39	35	32
5	53	51	49	44	41
6	65	63	61	57	53
7	76	75	73	69	65
8	91	89	87	83	80
9	108	106	104	101	98
10	130	128	126	121	118
11	151	150	149	143	140
12	178	175	172	168	165
13	208	206	204	200	196
14	238	236	235	229	226
15	275		269	264	260
16	309		302	300	295
17	345		339	337	331
18°	368	367	365	363	362

$g_\odot$	$\lambda=0,58\ \mu$	$\lambda=0,60\ \mu$	$\lambda=0,65\ \mu$	$\lambda=0,70\ \mu$
0°	10	8	6	4
1	14	12	9	7
2	18	16	13	10
3	23	21	18	15
4	30	28	25	22
5	39	37	35	32
6	50	49	46	43
7	63	62	59	56
8	78	77	74	70
9	96	94	91	87
10	116	114	110	106
11	138	136	132	126
12	164	161	156	150
13	194	192	186	180
14	223	222	219	218
15	257	256	254	249
16	292	290	288	285
17	327	325	322	318
18°	361	361	360	359

15° of submergence nighttime conditions begin to establish themselves.

The observed characteristics of the energy distribution in the spectrum of the twilight sky are dependent not only upon the presence of ozone but also upon the general conditions of light absorption in the Earth's atmosphere. A particularly strong influence on the formation of the observable spectrum of the twilight sky is exerted by the altitude of the so-called effective twilight rays at different degrees of solar submergence and different wavelengths. These altitudes were secured graphically from curves of the quantity of light scattered per unit volume of the terrestrial atmosphere, plotted as a function of height above the surface of the Earth.

As evidenced by the data in Table 8 and Fig. 10, at small submergences of the Sun the difference in altitude of the effective twilight ray for λ = 370 and λ = 700 mμ reaches 20 km. Inasmuch as at a given instant the effective twilight ray for short-wave radiation proves to be higher than for that of greater wavelength, the spectral distribution is liable to be of lower intensity in the extreme blue part of the spectrum as compared with the distribution corresponding to Rayleigh scattering. Furthermore, since at increasing angles of solar submergence the difference in altitudes of the effective twilight rays decreases (as illustrated by Fig. 10), the relative intensity of the blue radiation increases and, consequently, the above examined light intensity ratios between blue and yellow-green rays are bound to increase, too.

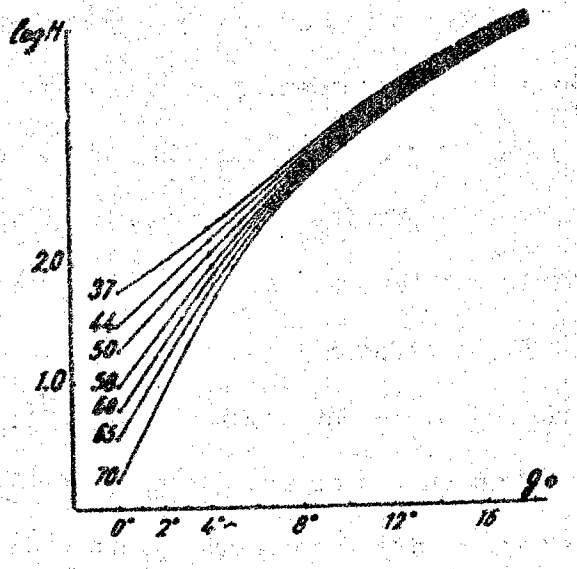

Fig. 10. Logarithm of the height of the twilight ray as a function of the solar submergence for different wavelengths.

The relatively large effective height of the twilight ray for the wavelength $\lambda = 370$ mμ is to be held responsible for the low values of twilight sky brightness computed for this wavelength (v. Fig. 7). Yet, the observed values at the same wavelength proved markedly higher than the computed values (v. Figs. 3 and 7). This difference is attributable to the strong effect of scattering of the higher orders in the case of such short wavelengths. An analysis of the optical properties of the Earth's atmosphere by the twilight investigation method has to take account of the fact that the rays of various wavelength supply information about different levels of the Earth's atmosphere at one and the same instant. Furthermore, one has to bear in mind that the width of the twilight rays differs for the different wavelengths. In this

respect, preference should be given to blue rays, in which the twilight ray is substantially narrower than in red rays.

References

1. R. Grandmontagne, Compte Rendu, 207, 1436, 1938.
2. J. Dufay, J. Gauzit, Annales des Astrophysiques, No 3 - 4, 135, 1946.
3. P. P. Migrelishvili, DAN SSSR (Transactions, Ac. Sci. USSR), 53, No 2, 127, 1946.
4. N. B. Divari, "Izv. Strofiz. In-ta" (News of the Astrophys. Inst.) 5, 89, 1957.
5. K. Bullrich, Bericht des deutsch. Wetterdienstes, No 4, 1950.
6. E. V. Ashburn, Journal Opt. Soc. America, 43, No 9, 805, 1953.
7. E. V. Ashburn, Journal Geophys. Research, 57, 85, 1952.
8. M. Gadsden, Journal Atmos. and Terr. Phys.,10, No 3, 176, 1957.
9. E. O. Hulbart, Journal Opt. Soc. America, 43, No 2, 113, 1953.
10. V. I. Moroz, "Astronomicheskiy zhurnal" (Astronomical Journal), 23, no 5, 717, 1956.
11. C. W. Allen, Astrophysical Quantities, London, Athlon Press, 1955.
12. Atmosfera Zemli i planet (Atmosphere of the Earth and the planets) edited by Kopeyer, Izd. I. L. M. (Foreign Literature Press) p 65, 1951.
13. A. A. Prokof'yev, Atmosfernyi ozon (Atmospheric Ozone), Izd. AN SSSR (Publ. Ac. Sci. USSR), p 18, 1951.
14. F. S. Johnson, J. D. Purcell, R. Tousey and K. Watanabe, Journ. Geophys. Research, 57, No 2, 157, 1952.

SOME RESULTS OF MEASUREMENTS OF THE INDICATRICES OF SCATTERING AND THE POLARIZATION OF LIGHT IN THE GROUND LAYER OF THE ATMOSPHERE

Pp. 108 - 117

by T. P. TOROPOVA

The present work gives some of the results obtained in determining the absolute and relative indicatrices of the polarization of light in the ground layer of the atmosphere as well as the degree of polarization at different scattering angles.

The measurements of the indicatrices of scattering and of the degree of polarization were carried out by the photoelectric method at the mountain observatory (1459 m above sea level) of the Astrophysical Institute of the Academy of Sciences of the Kazakh SSR. The photoelectric photometer, designed by a group of workers of the Institute /1/, consisted of an horizontal tube mounted on a bracket. The latter was capable of being rotated around its verticel axis with the aid of a system of cogwheels and worm gears driven by a motor. By means of a special relay, the photometer was automatically switched off and on by steps of 10°, its reading being recorded either on a galvanometer oscillograph (last variant) or a mirror galvanometer (first variant). As a pickup we used a FEU-19M photomultiplier connected with a quick-acting two-stage d.c. amplifier /2/.

Light filters were used to separate out a specified spectral region. The effective wavelength of the system optics-photomultiplier - filter was 495 mμ for observations conducted after August 15, 1958,

and 520 m μ for earlier observations (beginning of 1958 and end of 1957). A luminophor (representing a surface covered with a luminescent compound of steady action)was used for checking the sensisitiveness of the apparatus during the operations, its reading being recorded at the beginning and end of the observations. The optics of the photometer consisted of two lenses, the distance between which was equal to the sum of their focal lengths (Fabri's system /1/).

The FEU - 19 M photomultiplier was placed behind the optical system. It was fed from a high-voltage electronically stabilized VVS-1 rectifier supplying an output voltage of 500 to 1000 v at a current load of 100 ma.

Sufficient stability of the current voltage feeding the photomultiplier was maintained by means of twofold stabilization,viz., by interpolating an electromagnetic voltage stabilizer of the type SNE - 320 - 0.5 between the power source and the high-voltage VVS-1 rectifier. Such a twofold stabilization method made it possible to maintain the input voltage of the photomultiplier with an accuracy of the order of 0.01 to 0.02% which, in turn, ensured a degree of stability of the photomultiplier amplification to within 1 to 0.2%.

In the concluding tests, the capacity of the projection apparatus creating a parallel beam of light /1/ was slightly increased by means of replacing the original 500 w cinematic lamps by two lamps connected in series. Both these lamps were placed close to the focal point of the condenser lens (focal length: 3.42 m). For controlling and regula-

ting the current feeding the projector lamps, we inserted an ammeter of the first class and a sliding contact rheostat which helped to keep the circuit stable during the observations.

The tape of the galvanometer oscillograph was checked by means of a PKh - type meter. It is true that the accuracy of the intensity measurements is restricted by the small width of the oscillograph tape. However, by varying the range of amplification during the measurements at different angles of scattering, it is possible in all cases to obtain a perceptible reading on the oscillograph tape, which permits of performing the intensity measurements with an accuracy of about 3%. The linearity of the photoluminescence of the apparatus (i.e., the proportionality of the photocurrent of its illuminance) was checked by way of measuring the brightness of a light source with three neutral filters and without filter. For this purpose we utilized the three neutral filters NS-10 (NS-3 and) NS-7 of the small-size type No. 228, having a thickness of 2 mm and an optical density of 2.00, 0.84 and 0.26, respectively. In a graphical representation, with the logarithm of the intensity plotted on the axis of the abscissae, and the corresponding optical densities on that of the ordinates, a linear course of the photometer scale is bound to result in a straight line. Fig. 1 shows such a graph obtained on the basis of two series of measurements. In the absence of a filter (fourth point) the optical density is equal to zero. As is seen from this Figure,

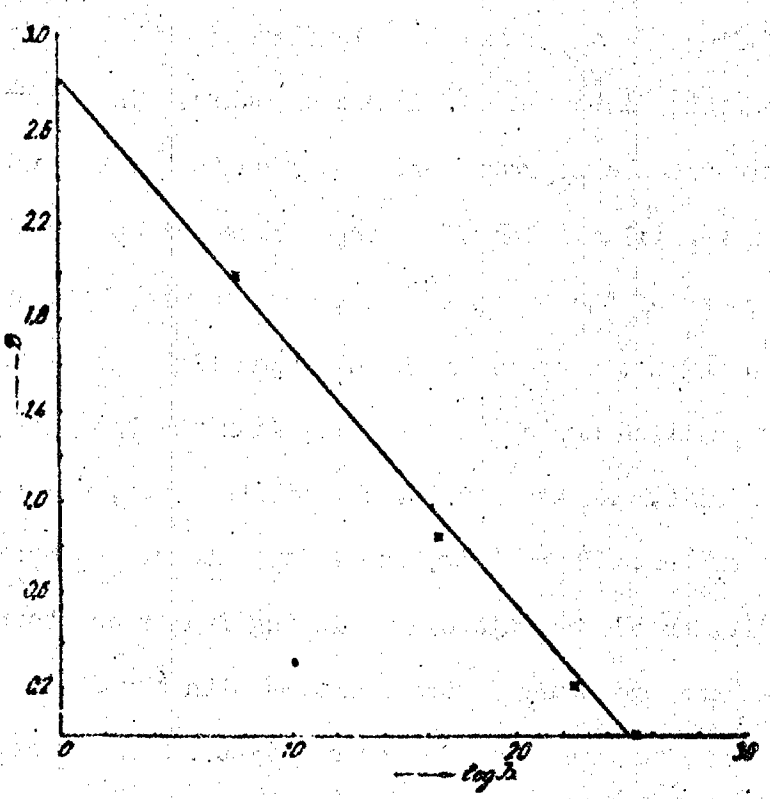

Fig. 1

the distribution of the points along the straight line is satisfactory. Hence, the linearity of the photometer scale readings in the range of the intensities measured may be regarded as proven.

The method of measuring the light-scattering indicatrices consisted in either recording the intensity of the light scattered from the projected beam of light, at different scattering angles, by steps of from 10 to 20° on the tape of the galvanometer oscillograph or taking the intensity readings with the help of the PS - 26 mirror galvanometer.

In determining the degree of polarization of the scattered light we placed in front of the inlet lens a polaroid fitted for being fixed in three positions distanced 60° from each other. The absence of light polarization in the apparatus was verified in the following way. The photometer was illuminated with nonpolarized light. To this end, the inlet aparture of the photometer was covered with two layers of tracing cloth and was exposed to the diffused light prevailing in the observation pavilion during the daytime, with the top untightly closed to leave a slit. As shown by P. N. Boiko's tests, tracing cloth is a good depolarizer. Thereafter, the light intensities were measured at three positions of the polaroid differing from each other by 60°. In this case, the photocurrent was measured with the PS-26 mirror galvanometer. If there is polarization of light in the apparatus, the readings taken must differ from each other. The results of six series of these measurements are set forth in Table 1 (the last line gives the mean values of all the series). The data stated show that the polarization in the apparatus does not exceed the measurement error.

Table 1

Polaroid position	1	2	3
Galvanometer readings	32	32	30
	40	40	40
	43	43	43
	37	37	39
	42	43	43
	53	53	52
Mean reading values	41	41	41

In order to determine the absolute scattering indicatrices, i.e., the luminous flux scattered per unit volume per unit of the solid angle expressed in units of the incident flux, we measured the brightness of a standard screen illuminated by the projected beam of light, whose albedo was known. Then the absolute indicatrice of scattering is determined from the Expression

$$\mu(\theta) = \frac{B(\theta)}{B_{(\omega)_{screen}}} \frac{A}{\pi h \cdot \cos z},$$

where B (θ) is the brightness of the scattered light in the direction θ ; B_{screen} is the brightness of the standard screen with known albedo A; z is the angle between the photometer axis and the normal to the projected beam; h is the beam width.

The results of measuring the indicatrices are partially reported in ref. /1/. However, in that work we took as the asymmetry characteristic of the indicatrices of scattering a rather arbitrary quantity, viz., the ratio of the intensity of scattering at an angle of 10° to that of

140°. To promote comparability of our data with theory and with those of other authors, we computed in the present work the asymmetry coefficients of the fluxes η which are determined by the ratio of the flux scattered in a "forward" direction, i.e., toward scattering angles below 90°, to the flux scattered "backward", i.e., toward the region of angles above 90°.

$$\eta = \frac{\int_0^{\frac{\pi}{2}} \mu(\theta) \sin\theta \, d\theta}{\int_{\frac{\pi}{2}}^{\pi} \mu(\theta) \sin\theta \, d\theta}, \qquad (1)$$

Both the numerator and the denominator of Expression (1) are determined by the method of numerical integration (trapeze method, in which $d\theta$ was taken to equal 10°). The values of the coefficient η for the different observation days are given in Table 2, column 1.

In order to clarify the part played by atmospheric aerosols in the scattering of light in the ground layer of the atmosphere, the aerosol indicatrix of scattering was separated out for each day of observation. For this purpose, the theoretically computed Raleigh indicatrix was subtracted from the absolute indicatrix obtained directly from the observations.

As is known, the Raleigh light scattering coefficient α_R, showing what part of the flux is scattered per unit volume in the direction θ

within the unit solid angle in the presence of a molecular atmosphere, is determined in the following manner:

$$\alpha_R = \frac{\pi^2 (n^2 - 1)^2}{2 N \lambda^4} (1 + \cos^2 \Theta),$$

where N is Loschmidt's number; λ is the wavelength of light in cm; n is the coefficient of air regraction. In calculating the Raleigh scattering indicatrix, we assumed $n-1 = 0.000293$; $N = 2.687 \times 10^{13}$.

We then calculated the scattering coefficients per unit air volume for the different observation days and compared them with the value for the Raleigh atmosphere. The coefficients were determined by way of integrating the absolute values of the scattering indicatrices over all angles of scattering

$$\alpha = 2\pi \int_0^{\pi} \mu(\theta) \sin \Theta \, d\Theta.$$

As a result of these calculations it was found that the scattering coefficients of the real atmosphere exceeded those of the Raleigh atmosphere 1.5 to 15 times. It follows from this that if the scattering coefficient for the ground layer of the atmosphere, as determined from observational data, is taken as 100%, the aerosol scattering is found to be between 60 and 94%.

On the basis of the aerosol indicatrices we were able to determine the asymmetry coefficient of the fluxes for the aerosol scattering, η_a, in strict analogy to the calculation of η from Expression (1). The values of the coefficients so determined are stated in Table 2, column 2.

Column 3 of Table 2 gives the ratios of the coefficients of scattering per unit volume of the atmospheric air, α, to the coefficients of scattering in the Raleigh atmosphere, α_R.

The least value obtained by us for the asymmetry coefficient of the aerosol indicatrix is 1.69 as on 9.9.1958. The largest coefficient ($\eta_a = 15.24$) was found for 10.11.1957. Observations on 9.9.1958 were preceded by slight precipitations, so the large particles were presumably washed out. Those on 10.11.1957 were followed by precipitations; the observation journal for that day notes low-lying continuous claudiness and a few drops of rain falling toward the end of the observations, the relative humidity being close to 100%. On the night of 11/12 October there were precipitations. In this case, most probably, the light scattering occurred in the presence of relatively large moist aerosols.

Appreciable asymmetry coefficients of the aerosol indicatrices of scattering were also found on 16 and 17 October 1957 and on 22 January 1958. The following notes are found in the journal for these days.

10.16. Clear. Soil still moist after precipitations of 10.12. Projected beam clearly visible against the sky. Mountains snow-covered.

10.17. Clear.Beam appears less bright than on the day before.

Thus, on 16 and 17 October, too, the scattering occurred in the presence of moist aerosols. The same applies to 1.22.1958.

1.22. Clear. Deep snow. Beneath the observatory, town wrapped in mist. On 23, 24, 25 and 26 October — clear. No fog noted. Relatively small η_α values for these days.

10.3. Dry. Considerable dust. Specks of dust clearly visible in projected beam. Small η_α coefficient (3.87).

It is known from Shifrin's work /4/ that for an extremely large completely reflecting particle the asymmetry coefficient η_α does not exceed 3.05. It is to be assumed, therefore, that on 3 October the scattering particles consisted of specks of dust mixed with wet aerosols.

The mean value for the asymmetry coefficient obtained by us accords well with the asymmetry coefficient $\eta_\alpha = 6.41$ resulting from Bullrich's mean data for the indicatrices of scattering /5/.

Foitzik /6/ obtained for the visible spectral region a somewhat higher value for $\eta = 8.17$. A still larger value results from Siden-

topf's work /7/, viz.: η = 11.5. Analyzing the data in Table 3, it was not possible to find ... (Omission. Translator's note.). In some cases, e.g., on 7 and 8 September 1958, large values of the scattering coefficient correspond to small asymmetry coefficients η_α, and vice versa, e.g., on 10.17.1957. This contradicts to some extent the results reported by Foitzik, but aggrees well with those obtained by Ye. V. Pyaskovskaya-Fesenkova /8/ for the whole atmosphere. In /8/ the latter author points out that the indicatrix of scattering may have a different form for the same locality and at the same transparency factor; on the basis of substantial observational data, she proves the absence of a single-valued correlation between the transparency factor of the atmosphere and the luminous flux dispersed in the direction of small scattering angles.

The degree of polarization for the different angles of scattering was determined by V. G. Fesenkov's method /9/ which consists in measuring the intensities of scattered light at three positions of the polaroid at intervals of 60°. If these intensities be designated, respectively, by I_1, I_2 and I_3, the degree of polarization is determined from the Expression:

$$p = \frac{2\sqrt{I_1(I_1 - I_2) + I_2(I_2 - I_3) + I_3(I_3 - I_1)}}{I_1 + I_2 + I_3}$$

In order to evaluate the error in determining the degree of polarization, one has to find the error in determining the intensities I_1, I_2 and I_3.

The main sources of error in the determination of I include the

following:

1. Errors of the photoelectric method;

2. Errors occurring in recording the intensities on the tape of the galvanometer oscillograph (due to the inconsiderable width of the tape);

3. Errors due to brightness fluctuations of the projected beam.

The photoelectric method permits of measuring the intensity of scattered light to within 0.5 to 1 %.The accuracy of measuring the intensities recorded on the tape of the galvanometer oscillograph is of the order of from 2.5 to 3 %. It should be noted that the greater part of the material on the determination of the degree of polarization, published in the present work, was obtained in measuring the intensities by means of a PS-26 mirror galvanometer, with an accuracy of up to 1 %.

Brightness fluctuations in the projected beam could arise from two causes: (1) Changes in transparency of the bottom layer of the atmosphere; (2) Changes in the luminous flux due to variations in the light intensity of the lamps in the projector circuit. The current in the projector lamp circuit was kept stable to an accuracy of 0.5 %, which ensured stability in the beam intensity up to 1 %. In order to avoid an error in determining the degree of polarization occurring because of a possible gradual change of transparency during observation, each series of measurement was divided into six readings : I_1, I_2, I_3, I_3, I_2, I_1.

In determining the degree of polarization for each angle of scattering we took the mean of two I_1, I_2, I_3 values. Taking into consideration all that has been said above, it can be assumed that the relative error in the intensity determination is of the order of 3 to 4%. Hence, it is easy to evaluate the relative error in determining the degree of polarization also. It is of the order of 5 %. The data gathered concerning the degree of polarization on the basis of 20 days of observations carried out, chiefly, in the Fall of 1958 are summarized in Table 2.

Table 2

Date	η	η_a	$\frac{a}{a_R}$	Date	η	η_a	$\frac{a}{a_R}$
1957 r.				1958 r.			
15. IV	2,54		5,1	22. VIII	2,30	2,89	6,8
29. IV	2,12		9,0	6. IX	2,77	3,39	4,7
3. X	2,38	3,87	2,8	7. IX	3,10	3,64	10.4
11. X	7,97	15,24	7,3	8. IX	1,67	1,82	7,0
16. X	5,50	11,52	7,2	9. IX	1,57	1,69	5,2
17. X	2,82	14,88	1,5	11. IX	2,67	3,23	7,7
1958 r,							
22. I	8,75	13,37	15,1	12. IX	4,02	10,00	3,9
23. I	1,67	7,82	1,5	13. IX	1,90	2,09	8,40
24. I	2,95	4,06	4,1	Mean			
25. I	2,08	2,46	4,9	for	3,29	6,23	6,25
26. I	3,78	3,97	3,4	all			
				days			

As a result of the polarization measurements it was established that during the period of observation the degree of polarization fluctuated between 33 and 70 % for an angle of scattering of 90°. The dependence of the degree of polarization on the angle of scattering varies slightly for different days. In some cases it takes the shape of a

smooth curve culminating close to 90°; it is then satisfactorily representable by a function which is proportional to the square of the sine of the angle of scattering (Fig. 2, a), that is, symmetrical relative to the latter. In other cases, the symmetry is upset, mainly, in the region of scattering angles larger than 90° (which, probably, is attributable to the admixture of large guttate scattering particles). In the remaining cases, the maximum degree of polarization is shifted toward large angles of scattering.

Given the absolute indicatrix of scattering, it is not difficult to divide the scattering intensity for each angle into two components polarized in two mutually perpendicular directions. Indeed,

$$p = \frac{I_s - I_p}{I_s + I_p} \text{ and } \mu(\Theta) = I_s + I_p, \qquad (2)$$

where p is the degree of polarization; I_p is the intensity of the light polarized parallel tothe plane of the predominant oscillations of the electric vector; and I_s is the intensity of the light polarized perpendicularly to the plane of the predominant oscillations of this vector. Calculating the Equations (2) jointly, we find for I_s and I_p the following Expressions:

$$I_s = \frac{1}{2}\mu(\Theta)(1+p); \quad I_p = \frac{1}{2}\mu(\Theta)(1-p).$$

Such a procedure is equivalent to dividing the general indicatrix of scattering into two separate indicatrices in polarized and normal rays, respectively, as was carried out by Ye. V. Pyaskovskaya-Fesenkova for the whole atmosphere /10/.

Table 3

Date \ H	10	20	30	40	50	60	70	90	110	119	120	130	140	150	160
1958															
16. VIII	—	6%	5%	—	17%	—	37%	53%	—	67%	—	46%	—	6%	12%
19. VIII	—	—	—	—	—	—	—	63	—	64	—	—	—	—	—
20. VIII	4%	—	5	—	25	—	41	62	—	—	—	26	—	22	—
21. VIII	—	6	4	—	23	—	56	58	—	—	—	—	—	—	—
22. VIII	1	3	—	10	—	31%	—	75	—	—	—	57	—	—	—
5. IX	5	—	7	—	31	—	54	63	—	54	—	41	—	14	—
6. IX	3	—	13	—	34	—	50	60	—	53	—	32	—	14	7
7. IX	8	—	5	—	17	—	29	60	—	56	—	28	—	17	—
8. IX	6	2	—	18	—	39	—	63	—	65	—	32	—	15	—
9. IX	3	—	11	—	30		57	60		—	—	23	—	10	—
11. IX	5	—	9	—	26	—	45	60	—	59	—	35	—	12	2
12. IX	4	—	7	—	22	—	44	56	64%	48	—	39	—	10	8
13. IX	8	7	—	14	38	—	48	55	—	—	—	24	—	27	—
14. IX	1	2	5	12	19	—	39	55	—	—	—	—	—	—	—
15. X	—	7	6	8	21	—	47	67	—	—	—		—	—	—
16. X	5	7	—	9	—	22	44	44	—	—	43%		12%	—	3
17. X	4	5	3	7	—	27	52	54	58	—	35	—	36	—	7
20. X	—	4	—	10	—	18	42	46	47	—	32	—	—	—	—
1959															
8 III	5,5	0,9	2,9	0,7	3,4	14	12	56	61	43			18	1	6
Means	4,7%	4,9%	6,7%	11,0%	25,3%	25,2%	43,9%	58,1%	57,5%	56,5%	35,7%	34,8%	22,0%	13,4%	5,4%

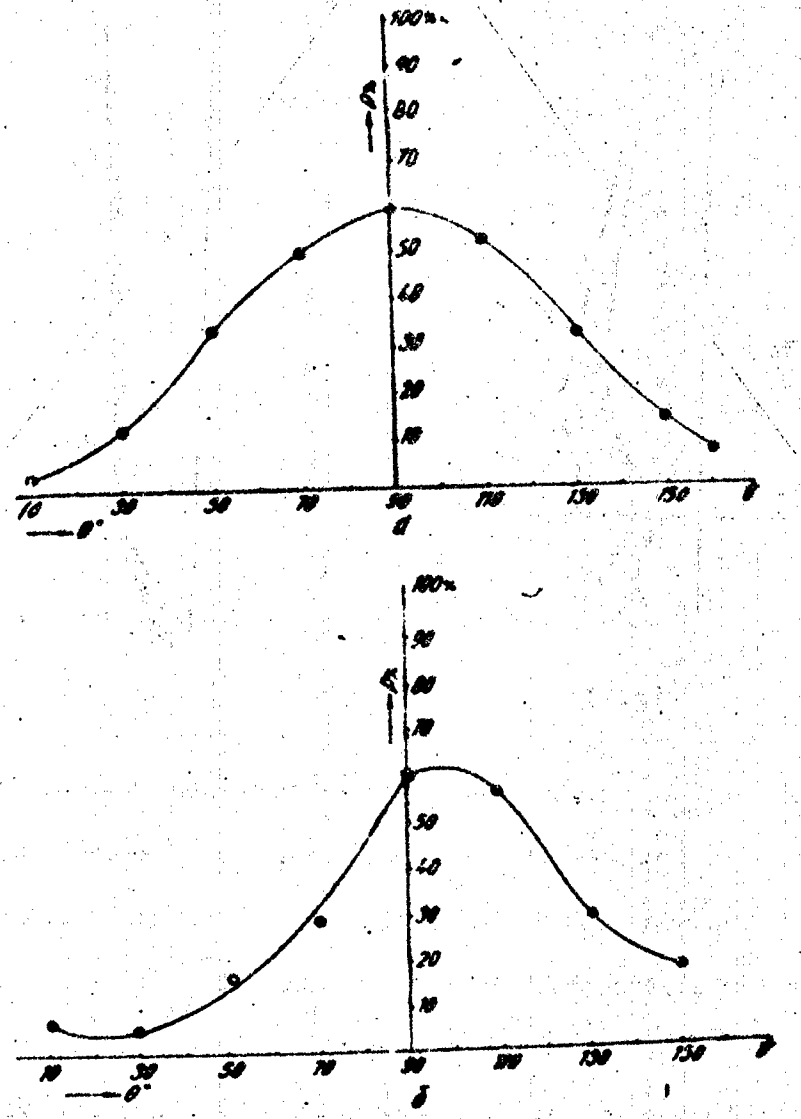

Fig. 2

In this way we plotted for each day of observation the I_s and I_p components as functions of the angle of scattering. The most typical of these curves are presented in Figs. 3 and 4.

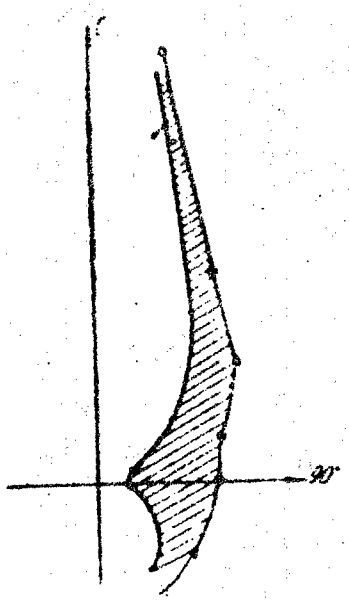

Fig. 3

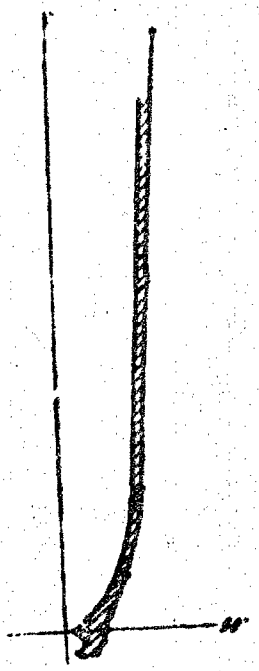

Fig. 4

In these Figures, the outer curves represent the I_s components, and the inner curves — the I_p components of scattering. Fig. 3 relates to 9 September 1958, being the day following precipitations, in which the large aerosols were washed out. The indicatrix of the light scattered in polarized and normal rays, plotted for this day, resembles those obtained by Ye. V. Pyaskovskaya-Fesenkova for the atmosphere as a whole.

References

1. P. N. Boiko, G. Sh. Lifshits, T. N. Toropova : DAN SSSR (Proceedings of Ac. Sci. USSR), 124, 4, 803, 1959.

2. V. I. Moroz: Apparatus and Experimental Technique, 1, 63,1956.

3. P. N. Boiko : News of the Astrophys. Inst., 8, 1958.

4. K. S. Shifrin: Rasseyanye sweta v mutnoi srede (Light Scattering in a Turbid Medium), Moscow-Leningrad, 1951.

5. K. Bullrich : Met. Z., Bd. 7, H.1 (1953) 1-19.

6. Foitzik and Zschaeck : Met. Z., Bd.7, H. 1,(1953) 1-19.

7. E. Reger and H. Sidentopf : Optik 1 (1946), 15-41.

8. Ye. V. Pyaskovskaya-Fesenkova : Issledovanye rasseyaniya sweta v zemnoi atmosfere (Investigation of the Scattering of Light in the Terrestrial Atmosphere). Ac. Sci. Press USSS, Moscow, 1957.

9. V. G. Fesenkov : Astronomicheskiy zhurnal (Astronomical Journal) , 1958, 35, 5, 681.

10. Ye. V. Pyaskovskaya-Fesenkova : DAN SSSR, 123, 6, 1006, 1958.

T H E E N D

2175